

# Investigation of the temperature dependence of the Casimir force between real metals

G. L. Klimchitskaya\* and V. M. Mostepanenko†

*Physics Department, Federal University of Paraíba, C.P.5008,  
CEP 58059-970, João Pessoa, Pb—Brazil*

## Abstract

We investigate the Casimir force acting between real metals at nonzero temperature. It is shown that the zero-frequency term of Lifshitz formula has interpretation problem in the case of real metal described by Drude model. It happens because the scattering theory underlying Lifshitz formula is not well formulated when the dielectric permittivity takes account of dissipation. To give the zeroth term of Lifshitz formula the definite meaning different prescriptions were used recently by different authors with diverse results. These results are shown to be improper and in disagreement with experiment and the general physical requirements. We propose the new prescription which is a generalization of Schwinger, DeRaad and Milton recipe formulated earlier for ideal metals. On this base the detailed numerical and analytical computations of the temperature Casimir force are performed in configuration of two plane plates and a spherical lens (sphere) above a plate. The corrections due to nonzero temperature and finite conductivity found in the paper are in agreement with the limiting case of perfect metal and fit all experimental and theoretical requirements. Among other facts, the previous results obtained in frames of plasma model are confirmed. It appears they are the limiting case of Drude model computations when the relaxation parameter goes to zero. The comparison with the Casimir force acting between dielectric test bodies is made.

PACS: 12.20.Ds, 11.10.Wx, 12.20.Fv

---

\*On leave from North-West Polytechnical Institute, St.Petersburg, Russia. Electronic address: galina@fisica.ufpb.br

†On leave from A.Friedmann Laboratory for Theoretical Physics, St.Petersburg, Russia. Electronic address: mostep@fisica.ufpb.br

# I INTRODUCTION

The H.B.G. Casimir effect [1] predicted more than fifty years ago is one of the most interesting manifestations of zero-point vacuum oscillations of quantized fields. The Casimir effect implies that there is some force acting between two uncharged bodies closely spaced in the vacuum. This effect is purely of quantum origins. There is no such force in classical physics. Unique to the Casimir force is its strong dependence on shape, switching from attractive to repulsive as a function of the size, geometry and topology of the boundary. The force results from the alteration by the boundaries of the zero-point electromagnetic energy that pervades all of space as predicted by quantum field theory. Alternatively, the Casimir force can be described as the retarded electromagnetic interaction of atomic and molecular dipoles and was extended to forces between macroscopic dielectric bodies characterized by some dielectric constant [2].

In recent years the Casimir effect has attracted much attention because of numerous applications in quantum field theory, atomic physics, condensed matter physics, gravitation and cosmology, and mathematical physics (see monographs [3, 4, 5, 6] and references therein). New precision experiments have been performed on measuring the Casimir force between metallic surfaces [7, 8, 9, 10, 11, 12]. In Refs. [13, 14, 15] some promising applications of the Casimir effect were proposed for diagnostic in thin films and in nano electro-mechanical systems. Given the above reasons it is very important to understand the Casimir force between real materials including the effect of such influential factors as surface roughness, finite conductivity, and nonzero temperature.

Finite conductivity corrections to the Casimir force have long been investigated. They were calculated using plasma model [16, 17, 18] up to the first order in the relative penetration depth of the zero-point electromagnetic oscillations into the metal. In [19] more exact results up to the second order were obtained, and in [20] — up to the fourth order. In Refs. [21, 22] the finite

conductivity corrections to the Casimir force were computed using tabulated optical data for the frequency-dependent complex refractive index. For all separations between the test bodies larger than the effective plasma wavelength of the metal under study the results of [20] and [21, 22] are shown to be in good agreement. The effects of surface roughness in combination with finite conductivity were investigated in detail in [23] for the configuration of a sphere above a plate used in experiments [8, 9, 10, 11]. Roughness contributions to the Casimir effect (including origination of a lateral force) has been treated recently in [24, 25, 26, 27].

The action of nonzero temperature on the Casimir force between dielectric semispaces was taken into account in the Lifshitz theory [2, 16]. For perfect metals at nonzero temperature the Casimir force was calculated in [28, 29] within the limits of quantum field theory in terms of the free energy density of vacuum. There were apparent differences between the results of [2, 16] and [28, 29] which were resolved in [18]. As shown by Schwinger, DeRaad and Milton [18], to obtain the case of perfect conductor from the Lifshitz theory one must take the limit of infinite dielectric permittivity before putting the frequency equal to zero in the temperature sum. The results of [2, 16] adapted for the case of perfect metal and of [28, 29] are then in agreement. The temperature corrections to the Casimir force turned out to be negligible in the experiments [8, 9, 10, 11] where the measurements were performed in the separation range  $a < 1 \mu\text{m}$ . However, at  $a > 1 \mu\text{m}$ , as in [7], the temperature corrections make large contributions to the zero-temperature force between perfect conductors (e.g., for  $a = 5 \mu\text{m}$  the temperature correction in configuration of a spherical lens above a plate exceeds the zero-temperature force [30]).

The increased accuracy of the Casimir force measurements invites further investigation of the temperature corrections in case of real metals. Although from a conceptual point of view the Lifshitz theory provides a way of obtaining all the required results, the problem here is worse than it was with the

case of perfect metals. In [31] it was suggested to use the plasma model in order to describe the dielectric permittivity along the imaginary frequency axis in the Lifshitz formula for the Casimir force at nonzero temperature (note that in [16, 17, 18, 19, 20] the plasma model was applied for this purpose at zero temperature only). In Refs. [32, 33] the detailed calculations of the temperature Casimir force were performed in framework of the Lifshitz theory and the plasma model. It was shown that the temperature corrections are negligible at small separations where the finite conductivity corrections are very important. By contrast, at large separations finite conductivity corrections can be ignored, whereas the temperature corrections play an important role. In [32, 33] the transition region between these two asymptotic regimes was also investigated where the combined effect of nonzero temperature and finite conductivity is important and should be taken into account.

It is a common knowledge that at small frequencies the dielectric permittivity  $\varepsilon$  is proportional to  $\omega^{-1}$  as is given by the Drude model. Because of this, the Drude model is favoured over the plasma model (which implies  $\varepsilon \sim \omega^{-2}$ ) when calculating the Casimir force at nonzero temperature. The first attempts to calculate the nonzero temperature Casimir force between real metals based on the Lifshitz formula and Drude model were undertaken in [33, 34, 35, 36, 37]. They have led to distinct and unexpected results. It was found that the value of the transverse reflection coefficient  $r_2$  of the electromagnetic oscillations at zero frequency becomes indefinite when one describes the boundary made of real metal using the Drude model. In [34, 35] the value  $r_2 = 0$  has been adopted. This assumption leads to a nonphysical conclusion that the asymptotic Casimir force at high temperature in the case of real metals is two times smaller than for the case of ideal metal (without regard to the particular value of the conductivity of real metal). Also, as a result of assumption, made in [34, 35], there arise large negative temperature corrections at small separations which are linear in temperature. These corrections are not only unacceptable from the theoretical point of view but are

in a conflict with experimental data [38].

The other authors [36, 37] assumed the value  $|r_2| = 1$  at zero frequency using the prescription of [18] formulated for perfect metal and well known relation by Hagen and Rubens which is valid for real photons only [39, 40]. This assumption also leads to nonphysical conclusions, i.e. to linear (although positive) temperature corrections at small separations and to the absence of any finite conductivity corrections to the Casimir force for real metals starting from the moderate separations of several micrometers regardless of metal quality (note that the same assumption was accepted in the latest version of [38]).

The situation was clarified in [33] where the discontinuity of the transverse reflection coefficient as a function of frequency and photon momentum was demonstrated in the case of real metal described by the Drude model. According to [33] to clear away the ambiguity in the zero frequency term of Lifshitz formula arising due to this discontinuity it is necessary to use an alternative representation for it [18, 28]. This representation gives the possibility to redefine the zero-frequency term of Lifshitz formula in order to assign it the definite meaning for real metals in accordance with the usual physical requirements. In [33], however, the values of the Casimir force including nonzero temperature and finite conductivity in the framework of the Drude model were not computed. Thus, up to now, there is no plausible qualitative information on the Casimir effect between real metals including the temperature corrections. The need for such investigation is apparent when the experimental and technological applications of the Casimir force mentioned above are considered. It is also important that recently, the Casimir effect has been used to obtain stronger constraints on the constants of long-range interactions (including corrections to the Newtonian gravitational law) predicted by the unified field theories, supersymmetry, supergravity and string theory [30, 41, 42, 43, 44]. The reliable theoretical values of the Casimir force at nonzero temperature between real metals and the extent of their

agreement with experiment are of particular interest in order to obtain the strongest constraints.

In the present paper we propose a method which allows one to attribute a definite value to the term of Lifshitz formula at zero frequency for real metals as described by the Drude model. This method avoids the above mentioned contradictions and solves the problem in a physically consistent way. The detailed computations of the Casimir force between real metals at nonzero temperature are performed for the configuration of two plane parallel plates and a sphere (lens) above a plate in a wide separation range from  $0.1\text{ }\mu\text{m}$  to  $10\text{ }\mu\text{m}$ . It is shown that at small separations (low temperatures) the temperature corrections are small irrespective of whether the Drude or plasma model is used. In particular, no corrections to the force arise which would be linear in temperature, such as in [34, 35, 36, 37]. At large separations (high temperatures) there is some difference between the finite conductivity corrections to the temperature Casimir force obtained with the plasma and Drude models, although the corrections themselves are rather small. With decreasing relaxation parameter the results from both models coincide. Our results at large separations join smoothly with the increase of conductivity with the asymptotic values obtained for the perfect metal (this is not the case in [34, 35] where the asymptotic force for a real metal is two times smaller than for the perfect one). Also the non-physical results of [36, 37], according to which at large separations the finite conductivity corrections are absent in the case of real metals, are shown to be in error. Below the nonzero temperature Casimir force between the dielectric bodies is also computed and the distinctions between the cases of metallic and dielectric bodies are discussed. The obtained results are in agreement with the performed experiments. They establish the theoretical basis for new precise experiments on measuring the Casimir force.

The paper is organized as follows. In Sec. II the general formalism for the Casimir force between real metals at nonzero temperature is presented

for the configuration of two plane parallel plates. Here special attention is paid to the indefinite character and discontinuity of the zeroth term of the Lifshitz formula in case of the Drude model. The representation of this term is given which is in accordance with the general physical requirements. In Sec. III the same is done for the configuration of a sphere (lens) above a plate. Sec. IV is devoted to the numerical and analytical computations of the temperature Casimir force for the configuration of two plane parallel plates. Both the asymptotics of low and high temperatures are considered and also a transition region between them. Sec. V contains the results of analogous computations for the configuration of a sphere (lens) above a plate. In Sec. VI the case of dielectrical test bodies is considered and the Casimir force at nonzero temperature is found. In Sec. VII reader will find conclusions and discussion. Appendices I and II contain some details of the mathematical calculations.

## II TEMPERATURE CASIMIR FORCE BETWEEN TWO PLANE PARALLEL PLATES

The original Lifshitz derivation [2, 16] of the temperature Casimir force between two semispaces was based on the assumption that the dielectric materials can be considered as continuous media characterized by randomly fluctuating sources. The correlation function of these sources, situated at different points, is proportional to the  $\delta$ -function of the radius-vector joining these points. The force per unit area acting upon one of the semispaces was calculated as the flux of incoming momentum into the semispace through the boundary plane. This flux is given by the appropriate component of the stress tensor ( $zz$ -component if  $xy$  is the boundary plane). Usual boundary conditions on the boundary surfaces between different media were imposed on the temperature Green's functions. To exclude the divergences, the values of all the Green's functions in vacuum were subtracted from their values in

dielectric media. The other derivation of Lifshitz formula is based on the solution of Maxwell's equations with appropriate boundary conditions on the surfaces separating different media [45, 46, 47]. In this manner the allowed surface modes and a harmonic oscillator free energy of each mode can be determined. The total renormalized free energy is obtained by the summation over all modes and subtraction of the free energy of vacuum. The nonzero temperature Casimir force is finally given by the negative derivative of the renormalized free energy with respect to the distance between semispaces (at zero temperature this procedure is presented in detail in [22, 47]).

The modern derivation of Lifshitz formula [48] is based on the temperature field theory in Matsubara formulation. In case of a static Casimir effect the system is in thermal equilibrium. To describe it at nonzero temperature one should take the Euclidean version of the field theory with a field periodic in the time variable within the interval  $\beta = \hbar/(k_B T)$ , where  $T$  is temperature,  $k_B$  is the Boltzmann constant. To find the free energy in case of two semispaces the scattering problem on the  $z$ -axis perpendicular to the boundary planes is considered. An electromagnetic wave coming from the left in the dielectric is scattered on the air gap and there exist a transmitted and a reflected wave. Finally the free energy and the Casimir force is expressed in terms of the scattering coefficient on the imaginary axis. Calculating this coefficient for the problem of two semispaces (notated by an index  $ss$ ) with a frequency dependent dielectric permittivity  $\varepsilon(\omega)$  separated by a gap of width  $a$  one finally obtains the Casimir force in the form [48]

$$F_{ss}(a) = -\frac{k_B T}{2\pi} \sum_{l=-\infty}^{\infty} \int_0^{\infty} k_{\perp} dk_{\perp} q_l \left\{ [r_1^{-2}(\xi_l, k_{\perp}) e^{2aq_l} - 1]^{-1} + [r_2^{-2}(\xi_l, k_{\perp}) e^{2aq_l} - 1]^{-1} \right\}, \quad (1)$$

where  $r_{1,2}$  are the reflection coefficients with parallel (perpendicular) polarization respectively given by

$$r_1^{-2}(\xi_l, k_{\perp}) = \left[ \frac{\varepsilon(i\xi_l)q_l + k_l}{\varepsilon(i\xi_l)q_l - k_l} \right]^2, \quad r_2^{-2}(\xi_l, k_{\perp}) = \left( \frac{q_l + k_l}{q_l - k_l} \right)^2. \quad (2)$$

Here  $\mathbf{k}_\perp$  is the momentum component lying in the boundary planes,  $k_\perp = |\mathbf{k}_\perp|$ ,  $\omega = i\xi$ , and the following notations are used

$$q_l = \sqrt{\frac{\xi_l^2}{c^2} + k_\perp^2}, \quad k_l = \sqrt{\varepsilon(i\xi_l) \frac{\xi_l^2}{c^2} + k_\perp^2}, \quad \xi_l = \frac{2\pi l}{\beta}. \quad (3)$$

Introducing a new variable  $p$  according to

$$k_\perp^2 = \frac{\xi_l^2}{c^2}(p^2 - 1) \quad (4)$$

we rewrite Eq. (1) in the original Lifshitz form [2, 16, 49]

$$F_{ss}(a) = -\frac{k_B T}{\pi c^3} \sum_{l=0}^{\infty}' \xi_l^3 \int_1^{\infty} p^2 dp \left\{ \left[ \left( \frac{K(i\xi_l) + \varepsilon(i\xi_l)p}{K(i\xi_l) - \varepsilon(i\xi_l)p} \right)^2 e^{2a\frac{\xi_l}{c}p} - 1 \right]^{-1} \right. \\ \left. + \left[ \left( \frac{K(i\xi_l) + p}{K(i\xi_l) - p} \right)^2 e^{2a\frac{\xi_l}{c}p} - 1 \right]^{-1} \right\}, \quad (5)$$

where

$$K(i\xi_l) \equiv [p^2 - 1 + \varepsilon(i\xi_l)]^{1/2} \quad (6)$$

and the prime near the summation sign means that the zeroth term is taken with the coefficient 1/2.

Note that the representation of Eq. (5) for the nonzero temperature Casimir force has a disadvantage as the  $l = 0$  term in it is the product of zero by a divergent integral. This is usually eliminated [49] by introducing the variable  $y$  instead of  $p$

$$y = |\tilde{\xi}_l| p, \quad \tilde{\xi}_l = 2a \frac{\xi_l}{c}, \quad (7)$$

where  $\tilde{\xi}_l$  is the dimensionless frequency. In terms of new variables Eq. (5) is

$$F_{ss}(a) = -\frac{k_B T}{16\pi a^3} \sum_{l=-\infty}^{\infty} \int_{|\tilde{\xi}_l|}^{\infty} y^2 dy \left\{ [r_1^{-2}(\tilde{\xi}_l, y) e^y - 1]^{-1} \right. \\ \left. + [r_2^{-2}(\tilde{\xi}_l, y) e^y - 1]^{-1} \right\}, \quad (8)$$

where

$$r_1(\tilde{\xi}_l, y) = \frac{\varepsilon y - \sqrt{(\varepsilon - 1)\tilde{\xi}_l^2 + y^2}}{\varepsilon y + \sqrt{(\varepsilon - 1)\tilde{\xi}_l^2 + y^2}}, \quad (9)$$

$$r_2(\tilde{\xi}_l, y) = \frac{y - \sqrt{(\varepsilon - 1)\tilde{\xi}_l^2 + y^2}}{y + \sqrt{(\varepsilon - 1)\tilde{\xi}_l^2 + y^2}}, \quad \varepsilon \equiv \varepsilon(i\xi_l) = \varepsilon \left( i \frac{c \tilde{\xi}_l}{2a} \right).$$

Both changes of variables (4) and (7) are, however, singular at  $l = 0$ . In fact (8) can be obtained from (1) by the regular change of variable

$$4a^2 k_{\perp}^2 = y^2 - \tilde{\xi}_l^2. \quad (10)$$

Because of this, the equivalent representations of Lifshitz formula (1) and (8) are preferred as compared to (5).

To calculate the Casimir force at nonzero temperature between real metals one should substitute the appropriate values  $\varepsilon(i\xi_l)$  into Eq. (1) or (8). In some frequency range  $\varepsilon(i\xi_l)$  can be found by the use of optical tabulated data for the complex refractive index for the metal under consideration tabulated in, e.g., [50] (this was done in [21, 22]). But in any case the optical data should be extrapolated outside the region where they are available in the tables to smaller and larger frequencies. This can be performed by the use of plasma model function

$$\varepsilon_p(i\xi) = 1 + \frac{\omega_p^2}{\xi^2} \quad (11)$$

or more exact Drude model one

$$\varepsilon_D(i\xi) = 1 + \frac{\omega_p^2}{\xi(\xi + \gamma)}, \quad (12)$$

where  $\omega_p$  is the plasma frequency and  $\gamma$  is the relaxation frequency. For some metals, the model dielectric functions with appropriate values of  $\omega_p$  and  $\gamma$  can be reliably used throughout the whole spectrum. Calculations of this type were performed in [32, 33, 34, 35, 36, 37] with different results. As shown below, the reason for this is the discontinuity of the transverse reflection coefficient  $r_2$  at zero frequency with respect to relaxation parameter which must be made continuous in a physically reasonable way in order to describe real metals by the Lifshitz formula.

If we put  $\xi_l = 0$  in Eqs. (2), (3) and use the plasma model dielectric function (11) the result is [32, 33]

$$r_1^2(0, k_{\perp}) = 1, \quad r_2^2(0, k_{\perp}) = \left( \frac{k_{\perp} - \sqrt{k_{\perp}^2 + \frac{\omega_p^2}{c^2}}}{k_{\perp} + \sqrt{k_{\perp}^2 + \frac{\omega_p^2}{c^2}}} \right)^2. \quad (13)$$

In the case of the Drude model dielectric function (12) it holds

$$\varepsilon_D(i\xi_l) \frac{\xi_l^2}{c^2} \Big|_{l=0} = 0, \quad (14)$$

which leads to [35]

$$r_1^2(0, k_\perp) = 1, \quad r_2^2(0, k_\perp) = 0 \quad (15)$$

for any  $k_\perp \neq 0$ . Note that (15) is valid for arbitrary small  $\gamma$  and arbitrary large  $\omega_p$ . Thus the second equation from (15) is in contradiction with the limiting case of ideal metal  $r_2^2(0, k_\perp) = 1$  which follows from (13) in the limit  $\omega_p \rightarrow \infty$ . The results obtained using (15) are in conflict with the known results for ideal metal [18, 29]. What is more important, the second equation of (15) does not approach the second equation of (13) when the relaxation frequency  $\gamma$  goes to zero. In the limit  $\gamma \rightarrow 0$  one still has  $r_2^2(0, k_\perp) = 0$ , not (13), although  $\lim_{\gamma \rightarrow 0} \varepsilon_D = \varepsilon_p$  in accordance with Eqs. (11), (12). In Secs. IV, V the discontinuity of the zero frequency term of the Lifshitz formula with respect to the relaxation parameter will be discussed in detail when comparing the continuous modification of this term as suggested below. Exactly the same results, as in (13), (15), are obtained if one uses the variables  $(\tilde{\xi}, y)$  instead of  $(\xi, k_\perp)$  and the representation (8) of the Lifshitz formula.

If the original representation (5) of the Lifshitz formula is exploited and written in terms of the variables  $(\xi, p)$  the situation changes drastically. Here one immediately arrives at

$$r_1^2(0, p) = r_2^2(0, p) = 1 \quad (16)$$

for all  $p \neq \infty$  irrespective of whether the plasma or Drude model is used for the dielectric permittivity on the imaginary axis. The reason for the distinct value of  $r_2(0, p)$  is the singular character of the change of variables (4) when  $\xi_0 = 0$ . This change relates the single value of  $k_\perp = 0$  to all the finite values of  $p$ , and all the values of  $k_\perp \neq 0$  to a single point  $p = \infty$ . The values (16) for both reflection coefficients at zero frequency were postulated at [36, 37] and used in all the numerical computations even after one more singular change

of variables (7) was performed in order to calculate the divergent integral in Eq. (5). We show below, that this postulate, though it works good for the perfect metal, is not justified for real metals of finite conductivity.

In actual truth, the transverse reflection coefficient  $r_2$  from Eq. (2) or (9) has a discontinuity as a function of two continuous variables ( $\tilde{\xi}$  and  $y$  for instance) in the case of the Drude dielectric function [33]. If one puts  $\tilde{\xi} = 0$  in (9) from the very beginning the result is  $r_2^2(0, y) = 0$  in agreement with (15). If, however, one approaches the point  $(\tilde{\xi} = 0, y = 0)$  along the direction  $\tilde{\xi} = ky$  in the  $(\tilde{\xi}, y)$ -plane then  $r_2^2(\tilde{\xi}, y) \rightarrow 1$ . The distinguishing feature of the Drude model is that for an arbitrarily small  $y$  there exists  $k$  such that  $r_2^2(ky, y)$  takes any value in between zero and unity. By contrast, in the case of plasma model both reflection coefficients are continuous, and  $r_2^2(ky, y)$  does not depend on  $k$  but is determined only by the value of  $y$ . Of even greater concern is that the transverse reflection coefficient at zero frequency is discontinuous with respect to the relaxation parameter  $\gamma$ .

As is seen from the above discussion, there is a serious unresolved issue concerning the value of the zero frequency term of the Lifshitz formula for real metals. In fact the scattering problem, which forms the basis of the Lifshitz formula, is meaningful only for nondissipative media (this is the case for plasma model or for dielectric materials). The case  $\varepsilon = \infty$ , as it is for metals at zero frequency, is especially complicated when the Drude model is used taking account of dissipation. The latter leads to the violation of the unitarity condition and thereby the zeroth term of Lifshitz formula becomes indefinite and must be redefined. For ideal metals of infinite conductivity this issue was resolved by the Schwinger, DeRaad, and Milton prescription [18] demanding that the limit  $\varepsilon \rightarrow \infty$  should be taken before setting  $\xi = 0$  (which is equivalent to the use of Eq. (16)). Let us find out, in what way the problem of zero-frequency term of the Lifshitz formula can be solved for real Drude metals in a physically satisfactory way.

For this purpose let us use the representation of the Lifshitz formula in

terms of continuous frequency variable. Such a representation was suggested in [28] and used in [18, 29] for the other purposes. According to the Poisson summation formula if  $c(\alpha)$  is the Fourier transform of a function  $b(x)$

$$c(\alpha) = \frac{1}{2\pi} \int_{-\infty}^{\infty} b(x) e^{-i\alpha x} dx \quad (17)$$

then it follows

$$\sum_{l=-\infty}^{\infty} b(l) = 2\pi \sum_{l=-\infty}^{\infty} c(2\pi l). \quad (18)$$

We apply this formula to Eq. (8) using the identification

$$b_{ss}(l) \equiv -\frac{k_B T}{16\pi a^3} \int_{|l|\tau}^{\infty} y^2 dy f_{ss}(l\tau, y), \quad \tau \equiv \frac{4\pi a k_B T}{\hbar c}, \quad (19)$$

where  $\tilde{\xi}_l = \tau l$  and

$$\begin{aligned} f_{ss}(l\tau, y) &= f_{ss}^{(1)}(l\tau, y) + f_{ss}^{(2)}(l\tau, y), \\ f_{ss}^{(i)}(l\tau, y) &= (r_i^{-2} e^y - 1)^{-1}, \quad i = 1, 2 \end{aligned} \quad (20)$$

are the even functions of  $l$ .

Then the quantity  $c_{ss}(\alpha)$  from Eq. (17) is given by

$$c_{ss}(\alpha) = -\frac{k_B T}{16\pi^2 a^3} \int_0^{\infty} dx \cos \alpha x \int_{x\tau}^{\infty} y^2 dy f_{ss}(x\tau, y). \quad (21)$$

Using Eqs. (8), (18), (21) one finally obtains the representation of the Lifshitz formula

$$\begin{aligned} F_{ss}(a) &= \sum_{l=-\infty}^{\infty} b_{ss}(l) \\ &= -\frac{\hbar c}{16\pi^2 a^4} \sum_{l=0}^{\infty} \int_0^{\infty} d\tilde{\xi} \cos \left( l\tilde{\xi} \frac{T_{eff}}{T} \right) \int_{\tilde{\xi}}^{\infty} y^2 dy f_{ss}(\tilde{\xi}, y), \end{aligned} \quad (22)$$

where the continuous frequency variable  $\tilde{\xi} = \tau x$ , and  $k_B T_{eff} = \hbar c / (2a)$ . Note that in the representation (22) the  $l = 0$  term gives the force at zero temperature. It is useful also to change the order of integration in Eq. (22)

$$F_{ss}(a) = -\frac{\hbar c}{16\pi^2 a^4} \sum_{l=0}^{\infty} \int_0^{\infty} y^2 dy \int_0^y d\tilde{\xi} \cos(l\tilde{\xi}t) f_{ss}(\tilde{\xi}, y), \quad (23)$$

where  $t \equiv T_{eff}/T$ .

Let us isolate the zero-frequency term of the usual Lifshitz formula (8) with discrete frequencies in representation (23). In this a way it will be expressed in terms of the integrals with respect to continuous variables  $\tilde{\xi}$ ,  $y$ . For this purpose we write out separately the terms of Eq. (23) with  $l = 0$ , integrate all the other terms by parts with respect to  $\tilde{\xi}$ , change the order of summation and integrations, and use the formula [51]

$$\sum_{l=1}^{\infty} \frac{\sin(lzt)}{l} = \frac{1}{2} \left[ \pi + 2\pi A \left( \frac{tz}{2\pi} \right) - tz \right], \quad (24)$$

where  $A(z)$  is the integer portion of  $z$ . The result of these transformations is

$$\begin{aligned} F_{ss}(a) = & -\frac{\hbar c}{32\pi^2 a^4} \left\{ \int_0^{\infty} y^2 dy \int_0^y d\tilde{\xi} f_{ss}(\tilde{\xi}, y) \right. \\ & + \frac{1}{t} \int_0^{\infty} y^2 dy f_{ss}(y, y) \left[ \pi + 2\pi A \left( \frac{ty}{2\pi} \right) - ty \right] \\ & \left. - \frac{1}{t} \int_0^{\infty} y^2 dy \int_0^y d\tilde{\xi} \frac{\partial f_{ss}(\tilde{\xi}, y)}{\partial \tilde{\xi}} \left[ \pi + 2\pi A \left( \frac{t\tilde{\xi}}{2\pi} \right) - t\tilde{\xi} \right] \right\}. \end{aligned} \quad (25)$$

Here the first term is the zero-temperature force. The second and the third contributions in the right-hand side of Eq. (25) can be transformed using the definition of the function  $A(z)$  and representation of  $f_{ss}$  in terms of the sum of parallel and transverse modes in accordance with (20). Taking into account that  $f_{ss}^{(1)}$  and its derivative are continuous functions (as distinct from  $f_{ss}^{(2)}$ ) one obtains finally after the cancellation of zero-temperature contribution (see Appendix I for details)

$$F_{ss}(a) = F_{ss}^{(l=0)}(a) - \frac{k_B T}{8\pi a^3} \sum_{l=1}^{\infty} \int_{\tilde{\xi}_l}^{\infty} y^2 dy f_{ss}(\tilde{\xi}_l, y). \quad (26)$$

In this equation all the terms with  $l \geq 1$  coincide with those in Eq. (8) and the term with  $l = 0$  is given by

$$\begin{aligned} F_{ss}^{(l=0)}(a) = & -\frac{k_B T}{16\pi a^3} \left\{ \int_0^{\infty} y^2 dy \left[ f_{ss}^{(1)}(0, y) + f_{ss}^{(2)}(y, y) \right] \right. \\ & \left. - \int_0^{\infty} y^2 dy \int_0^y d\tilde{\xi} \frac{\partial f_{ss}^{(2)}(\tilde{\xi}, y)}{\partial \tilde{\xi}} \right\}. \end{aligned} \quad (27)$$

The obtained representation for the zero-frequency term of the Lifshitz formula is well suited for solving the problem formulated above. In terms of dimensionless variables  $(\tilde{\xi}, y)$  the plasma and Drude dielectric functions take the form

$$\varepsilon_p(i\tilde{\xi}) = 1 + \frac{\tilde{\omega}_p^2}{\tilde{\xi}^2}, \quad \varepsilon_D(i\tilde{\xi}) = 1 + \frac{\tilde{\omega}_p^2}{\tilde{\xi}(\tilde{\xi} + \tilde{\gamma})}, \quad (28)$$

where  $\tilde{\omega}_p \equiv 2a\omega_p/c$ ,  $\tilde{\gamma} \equiv 2a\gamma/c$ . Evidently, no discontinuity problem arises in the single integral with respect to  $y$  in the right-hand side of Eq. (27). It is well defined for both dielectric functions of Eq. (28) and for both polarizations, and contains the limiting cases of an ideal metal and zero relaxation parameter. What this means is that the single integral term in (27) is analytic with respect to  $\tilde{\gamma}$ , i.e. its values calculated with the Drude model approach the values calculated with the plasma model when  $\tilde{\gamma} \rightarrow 0$  (see also the numerical computations of Sec. IV).

A completely different type of situation occurs in the double integral from the right-hand side of Eq. (27). In fact, by the use of (9), (20) one obtains

$$\frac{\partial f_{ss}^{(2)}(\tilde{\xi}, y)}{\partial \tilde{\xi}} = 2 \frac{e^y}{[e^y - r_2^2(\tilde{\xi}, y)]^2} r_2(\tilde{\xi}, y) \frac{\partial r_2(\tilde{\xi}, y)}{\partial \tilde{\xi}}, \quad (29)$$

where

$$\frac{\partial r_2(\tilde{\xi}, y)}{\partial \tilde{\xi}} = -\frac{2y}{\left[\sqrt{(\varepsilon - 1)\tilde{\xi}^2 + y^2} + y\right]^2} \frac{2\tilde{\xi}(\varepsilon - 1) + \tilde{\xi}^2 \frac{d\varepsilon}{d\tilde{\xi}}}{2\sqrt{(\varepsilon - 1)\tilde{\xi}^2 + y^2}}. \quad (30)$$

Substitution of  $\varepsilon = \varepsilon_p$  from Eq. (28) into (29), (30) leads to

$$\frac{\partial r_2(\tilde{\xi}, y)}{\partial \tilde{\xi}} = \frac{\partial f_{ss}^{(2)}(\tilde{\xi}, y)}{\partial \tilde{\xi}} = 0, \quad (31)$$

so that in the case of the plasma model the double integral in (27) vanishes. If, however,  $\varepsilon = \varepsilon_D$  is substituted into (29), (30) one discovers a discontinuity in  $\tilde{\gamma}$ . Actually, as it follows from (29), (30)

$$\lim_{\tilde{\gamma} \rightarrow 0} \frac{\partial f_{ss}^{(2)}(\tilde{\xi}, y)}{\partial \tilde{\xi}} = 0 \quad (32)$$

for any  $\tilde{\xi} \geq 0$  and  $y \neq 0$ . On the other hand,

$$\lim_{\tilde{\gamma} \rightarrow 0} \int_0^y d\tilde{\xi} \frac{\partial f_{ss}^{(2)}(\tilde{\xi}, y)}{\partial \tilde{\xi}} = \left[ \left( \frac{y + \sqrt{\tilde{\omega}_p^2 + y^2}}{y - \sqrt{\tilde{\omega}_p^2 + y^2}} \right)^2 e^y - 1 \right]^{-1} \neq 0. \quad (33)$$

To conclude, the presence of the double integral in the right-hand side of Eq. (27) renders it unsuitable for real metals described by the Drude model.

To remedy the situation let us notice that under the increase of  $\varepsilon$  it holds

$$\frac{\partial f_{ss}^{(2)}(\tilde{\xi}, y)}{\partial \tilde{\xi}} \sim \frac{1}{\sqrt{\varepsilon - 1}} \rightarrow 0 \quad \text{with } \varepsilon \rightarrow \infty. \quad (34)$$

Consequently, the discontinuous term can be deleted by the use of Schwinger, DeRaad and Milton-type prescription [18] which is that the limit of dielectric permittivity to infinity must be performed before setting frequency to zero when considering the zero-frequency term of the Lifshitz formula. For ideal metals the use of such a prescription is necessary in order to achieve agreement between the Lifshitz formula for dielectrics and field theoretical results obtained for a perfect metal, i.e. for boundaries with the Dirichlet boundary condition. As it is advocated here, for real metals the analogous prescription must be used in a more restricted way to eliminate the discontinuity in the zero-frequency term.

With the above prescription the Casimir force acting between two plane parallel plates at nonzero temperature is given by

$$F_{ss}(a) = -\frac{k_B T}{16\pi a^3} \left\{ \int_0^\infty y^2 dy [f_{ss}^{(1)}(0, y) + f_{ss}^{(2)}(y, y)] + 2 \sum_{l=1}^{\infty} \int_{\tilde{\xi}_l}^{\infty} y^2 dy f_{ss}(\tilde{\xi}_l, y) \right\}. \quad (35)$$

In Sec. IV the detailed calculations of the Casimir force using Eq. (35) are performed. The obtained results are compared with those obtained by other authors.

### III TEMPERATURE CASIMIR FORCE IN CONFIGURATION OF A SPHERICAL LENS (SPHERE) ABOVE A PLATE

In this section the most important results of Sec. II are adapted for a lens (sphere) above a semispace (plate) which is the configuration most often used in experiments [7, 8, 9, 10, 11]. Although there is no fundamental derivation of the Casimir force acting between a lens and a plate the proximity force theorem [52] gives the possibility to express it in terms of the Casimir free energy density for the configuration of two plane parallel plates. This latter is given by [32, 33, 48]

$$E_{ss}(a) = \frac{k_B T}{4\pi} \sum_{l=-\infty}^{\infty} \int_0^{\infty} k_{\perp} dk_{\perp} \left\{ \ln \left[ 1 - r_1^2(\xi_l, k_{\perp}) e^{-2aq_l} \right] + \ln \left[ 1 - r_2^2(\xi_l, k_{\perp}) e^{-2aq_l} \right] \right\}, \quad (36)$$

where the reflection coefficients and other notations are introduced in Eqs. (2), (3). Note that the Casimir force between plates from Eq. (1) can be obtained as  $F_{ss} = -\partial E_{ss}/\partial a$ .

According to the proximity force theorem [52] the Casimir force acting between a lens (sphere) of radius  $R$  and a plate is

$$F_{sl}(a) = 2\pi R E_{ss}(a) = \frac{k_B T R}{2} \sum_{l=-\infty}^{\infty} \int_0^{\infty} k_{\perp} dk_{\perp} \left\{ \ln \left[ 1 - r_1^2(\xi_l, k_{\perp}) e^{-2aq_l} \right] + \ln \left[ 1 - r_2^2(\xi_l, k_{\perp}) e^{-2aq_l} \right] \right\}. \quad (37)$$

Index  $sl$  here stands for semispace-lens. This formula is valid with rather high accuracy of about  $a/R$  [53] which is usually a fraction of a percent.

Introducing the dimensionless variables  $\tilde{\xi}_l$  and  $y$  from Eqs. (7), (10) we rewrite Eq. (37) in the form

$$F_{sl}(a) = \frac{k_B T R}{8a^2} \sum_{l=-\infty}^{\infty} \int_{|\tilde{\xi}_l|}^{\infty} y dy \left\{ \ln \left[ 1 - r_1^2(\tilde{\xi}_l, y) e^{-y} \right] + \ln \left[ 1 - r_2^2(\tilde{\xi}_l, y) e^{-y} \right] \right\}. \quad (38)$$

This result is in direct analogy with Eq. (8) for two plates. There is no need to use singular changes of variables as discussed in the previous section.

The term of Eq. (38) with  $l = 0$  suffers exactly the same ambiguity as the zeroth term of Eq. (8) if one uses the Drude model (12) to describe the dependence of a dielectric permittivity on frequency. This ambiguity lies in the fact that the quantity  $r_2^2(\tilde{\xi}, y)$  has a discontinuity at a point (0,0) as a function of two variables and is discontinuous also at the point of zero relaxation parameter (see the detailed discussion in Sec. II). Because of this, the zeroth term of Eq. (38), when applied to real metals, must be modified in the same way as it was done for configuration of two plane plates. For this purpose we apply the Poisson summation formula (18) and rewrite Eq. (38) in the form analogical to Eq. (22)

$$F_{sl}(a) = \frac{\hbar c R}{8\pi a^3} \sum_{l=0}^{\infty} ' \int_0^{\infty} d\tilde{\xi} \cos \left( l\tilde{\xi} \frac{T_{eff}}{T} \right) \int_{\tilde{\xi}}^{\infty} y dy f_{sl}(\tilde{\xi}, y), \quad (39)$$

where

$$\begin{aligned} f_{sl}(\tilde{\xi}, y) &= f_{sl}^{(1)}(\tilde{\xi}, y) + f_{sl}^{(2)}(\tilde{\xi}, y), \\ f_{sl}^{(i)}(\tilde{\xi}, y) &= \ln \left( 1 - r_i^2 e^{-y} \right). \end{aligned} \quad (40)$$

Evidently, the zeroth term of Eq. (39) gives us the Casimir force at zero temperature. The terms with  $l \geq 1$  represent the temperature correction. After changing the order of integration in Eq. (39) one obtains

$$F_{sl}(a) = \frac{\hbar c R}{8\pi a^3} \sum_{l=0}^{\infty} ' \int_0^{\infty} y dy \int_0^y d\tilde{\xi} \cos(l\tilde{\xi}t) f_{sl}(\tilde{\xi}, y). \quad (41)$$

Using Eq. (24) and performing exactly the same transformations as in Sec. II and Appendix I, the Casimir force between a plate and a lens takes the form

$$F_{sl}(a) = F_{sl}^{(l=0)}(a) + \frac{k_B T R}{4a^2} \sum_{l=1}^{\infty} \int_{\tilde{\xi}_l}^{\infty} y dy f_{sl}(\tilde{\xi}_l, y). \quad (42)$$

Here all terms with  $l \geq 1$  are exactly the same as in Eq. (38), whereas the

zeroth term is given by

$$F_{sl}^{(l=0)}(a) = \frac{k_B T R}{8a^2} \left\{ \int_0^\infty y dy \left[ f_{sl}^{(1)}(0, y) + f_{sl}^{(2)}(y, y) \right] - \int_0^\infty y dy \int_0^y d\tilde{\xi} \frac{\partial f_{sl}^{(2)}(\tilde{\xi}, y)}{\partial \tilde{\xi}} \right\}. \quad (43)$$

This representation of the zero-frequency term is in direct analogy with Eq. (27) for two plates. Like in (27), no discontinuity is contained in the single integral with respect to  $y$ . As to the double integral in (43), it is discontinuous with respect to the relaxation parameter  $\tilde{\gamma}$  at a point  $\tilde{\gamma} = 0$ . In fact, it follows from Eq. (40)

$$\frac{\partial f_{sl}^{(2)}(\tilde{\xi}, y)}{\partial \tilde{\xi}} = \frac{2r_2(\tilde{\xi}, y)}{e^y - r_2^2(\tilde{\xi}, y)} \frac{\partial r_2(\tilde{\xi}, y)}{\partial \tilde{\xi}}, \quad (44)$$

where the derivative of the transverse reflection coefficient was calculated in Eq. (30). Once again, in the case of plasma model the derivative (44), and also the double integral in (43), vanish. As to the Drude model, it follows from (44)

$$\lim_{\tilde{\gamma} \rightarrow 0} \frac{\partial f_{sl}^{(2)}(\tilde{\xi}, y)}{\partial \tilde{\xi}} = 0 \quad (45)$$

but

$$\lim_{\tilde{\gamma} \rightarrow 0} \int_0^y d\tilde{\xi} \frac{\partial f_{sl}^{(2)}(\tilde{\xi}, y)}{\partial \tilde{\xi}} = \ln \left[ 1 - \left( \frac{y - \sqrt{\tilde{\omega}_p^2 + y^2}}{y + \sqrt{\tilde{\omega}_p^2 + y^2}} \right)^2 e^{-y} \right] \neq 0, \quad (46)$$

which means the discontinuity of the double integral in (43) as a function of  $\gamma$ .

This discontinuity leads to the nonphysical results (see Secs. IV, V). It can be deleted by taking the limit of the dielectric permittivity to infinity prior to setting the frequency equal to zero in accordance with prescription used in Sec. II. Then due to (30), (44)

$$\frac{\partial f_{sl}^{(2)}(\tilde{\xi}, y)}{\partial \tilde{\xi}} \sim \frac{1}{\sqrt{\varepsilon - 1}} \rightarrow 0 \quad \text{with } \varepsilon \rightarrow \infty \quad (47)$$

and the discontinuous term in (43) disappears.

Using this prescription, one finally obtains the expression for the Casimir force acting between a plate and a spherical lens (sphere) at nonzero temperature

$$F_{sl}(a) = \frac{k_B T R}{8a^2} \left\{ \int_0^\infty y dy \left[ f_{sl}^{(1)}(0, y) + f_{sl}^{(2)}(y, y) \right] + 2 \sum_{l=1}^\infty \int_{\tilde{\xi}_l}^\infty y dy f_{sl}(\tilde{\xi}_l, y) \right\}. \quad (48)$$

The calculations of the Casimir force on the base of Eq. (48) are contained in Sec. V. The obtained results are compared with those obtained without the use of the above prescription [34, 35] or using another prescription [36, 37].

## IV COMPUTATIONS OF THE CASIMIR FORCE BETWEEN TWO PLATES MADE OF REAL METAL

We start the numerical computation of the Casimir force with Eq. (35) using the Drude and plasma dielectric functions (12). For the sake of definiteness, we consider the case of aluminum whose plasma frequency and relaxation parameter can be chosen as follows [50]

$$\begin{aligned} \omega_p &\approx 12.5 \text{ eV} \approx 1.9 \times 10^{16} \text{ rad/s,} \\ \gamma &\approx 0.063 \text{ eV} \approx 9.6 \times 10^{13} \text{ rad/s.} \end{aligned} \quad (49)$$

The most descriptive quantity illustrating the temperature correction to the Casimir force is

$$\delta_T(F_{ss}^f) = \frac{F_{ss}^f(a, T_0) - F_{ss}^f(a, 0)}{F_{ss}^f(a, 0)}. \quad (50)$$

Here the upper index  $f$  near the quantity  $F_{ss}$  from Eq. (35) signifies one or another dielectric function (Drude or plasma for instance), and the second argument  $T_0 = 300 \text{ K}$ , and  $T = 0$  means the temperature at which the Casimir force is computed. The relative temperature correction (50) is a function of separation  $a$ . It incorporates effectively both the case of low temperatures

(which occurs when  $T_0 \ll T_{eff}$  at small  $a$ ) and high temperatures (as  $T_0 \gg T_{eff}$  at large  $a$ ).

The results of numerical computations by Eqs. (35), (50) in the case  $f = D$  (Drude model) are presented in Fig. 1 by the solid curve 1. In the same figure the solid curve 2 illustrates the result obtained for dielectric plates (this case is discussed in Sec. VI). The dashed curve represents the result obtained by the approach of [34, 35]. In accordance with this approach, as was discussed in Sec. II, one should substitute  $f_{ss}^{(2)}(0, y) = 0$  instead of  $f_{ss}^{(2)}(y, y)$  into Eq. (35).

As is seen from Fig. 1 (curve 1), in the case of real metals the relative temperature correction is rather small at small separations and monotonically increases with the increase of separation remaining positive as it should be from general thermodynamical considerations. In contrast to this, the temperature correction, computed on the basis of [34, 35], is negative in a wide range of separations and turns into zero at a separation  $a \approx 6.3 \mu\text{m}$ . For larger distances it becomes positive. At small distances it is rather large by the modulus and increases linearly with distance (temperature). This behavior is in radical contradiction with both the case of ideal metal and a metal described by the plasma model dielectric function considered in detail in [32, 33]. At the same time the results obtained here are in good agreement with both limiting cases of an ideal metal and metal described by the plasma model.

Note that in the original paper [35] not  $\delta_T(F)$  but the correction factor was plotted as a function of separation  $a$ , i.e. the ratio between the Casimir force for real metals computed at  $T_0 = 300 \text{ K}$  and the Casimir force for ideal metals at zero temperature. According to the results of [32] in the case of plasma model this correction factor is approximately equal to the product of the correction factors through finite conductivity (at zero temperature) and through nonzero temperature (for the ideal metal). Thus the resulting negative temperature corrections, which are unacceptable from the thermodynamical point of view, were not clearly evident in [35].

In Table 1 the values of the relative temperature corrections are given at several distances between the plates in the case of Drude model (present paper, column 2), plasma model (present paper, column 3), for the ideal metal (column 4), computed on the base of [35] in frames of Drude model (column 5), and computed on the base of [36, 37] in frames of Drude and plasma models (columns 6 and 7 respectively). We remind that in [36, 37] all computations were performed by Eq. (5) where in the zeroth term the reflection coefficients (16) were substituted. As is seen from the comparison of columns 2–4, in the framework of the Drude model the relative temperature correction at smallest separations is three orders larger than with the plasma model and four orders larger than for the ideal metal. Note that for the ideal metal at small separations the lowest nonzero temperature correction to the zero-temperature result is of order  $(T/T_{eff})^4$  (see below). With increasing of separation the difference between the predictions of Drude and plasma models decreases approaching the values obtained for the ideal metal (column 4). At small separations the modulus of temperature correction calculated on the base of [35] (column 5) is several times larger than calculated by us (column 2) and the correction itself is negative. The results of the calculations on the base of [36, 37] (columns 6, 7) are also significantly different from our corresponding results of columns 2, 3. According to [36, 37] there exist large temperature corrections at small separations which are linear in temperature.

Now let us discuss the finite conductivity corrections to the Casimir force at nonzero temperature. They can be characterized by the quantity

$$\delta_c(F_{ss}^f) = \frac{F_{ss}^0(a, T_0) - F_{ss}^f(a, T_0)}{F_{ss}^0(a, T_0)}, \quad (51)$$

where, as above,  $F_{ss}^0(a, T_0)$  is the Casimir force between perfect metallic plates at temperature  $T_0$ . The results of numerical computations of  $\delta_c(F_{ss}^f)$  in the case of the Drude model ( $f = D$ ) are shown in Fig. 2. The solid curve represents the finite conductivity correction obtained by our method (Eq. (35)) at  $T_0 = 300$  K. For comparison the corresponding results at zero temperature  $T_0 = 0$  are given by the short-dashed curve. The long-dashed curve is

obtained at  $T_0 = 300$  K in the framework of the approach of [36, 37]. In Fig. 3 the results computed in the case of the plasma model ( $f = p$ ) are shown with the same notations as in Fig. 2. As is seen from Figs. 2, 3, in the Drude model the finite conductivity correction is larger than in the plasma model at all temperatures and at all separations. From Fig. 3 it follows that at  $a = 1 \mu\text{m}$  the finite conductivity correction computed using the plasma model at  $T_0 = 300$  K is practically the same as at  $T_0 = 0$ .

It is notable that the finite conductivity correction computed on the basis of [36, 37] turns into zero at separations larger than  $5 \mu\text{m}$  in both Drude and plasma models (see the long-dashed curves in Figs. 2 and 3). In fact, as is seen from the solid and short-dashed curves in Figs. 2, 3, with increasing temperature the finite conductivity correction decreases. The extent of this decrease depends on the model used ( $D$  or  $p$ ) and on the values of plasma and relaxation frequencies. In contrast to this, the finite conductivity correction computed on the basis of [36, 37] turns into zero at one and the same separation not only in different models but also for one and the same model with different values of parameters, i.e. regardless of the quality of metal under consideration. It is easily seen, that the separation value, at which the finite conductivity corrections of [36, 37] vanish, is determined not by the conductivity properties of a metal but by the smallness of terms with  $l \geq 1$  in the Lifshitz formula which are of order  $\exp(-2\pi T/T_{eff})$ . This means that the anzats used in [36, 37] to redefine the zeroth term of Lifshitz formula (see the above discussion in Sec. II) is unjustified.

It is of interest to consider the dependence of our results on the relaxation parameter  $\gamma$  of Drude model. In Fig. 4 the relative temperature correction computed by Eqs. (35), (50) is plotted with the decreasing of  $\gamma$  at a separation  $a = 2 \mu\text{m}$ , and at a temperature  $T_0 = 300$  K (solid curve). In the same figure the dashed curve represents the result obtained using the plasma model. It is clearly seen that with the decrease of  $\gamma$  by 3 orders of magnitude the results computed in the Drude model join smoothly with the results of the

plasma model as it should be from general considerations. Note that this is not the case in the approach of [34, 35] where the results obtained with the Drude model do not join the results of the plasma model with decreasing  $\gamma$ . The reason is that, different definitions of the zero-frequency term of Lifshitz formula are used in [34, 35] and in the present paper (see Sec. II).

As to the papers [36, 37], there is the smooth transition between the results obtained in Drude and plasma models. However, as was indicated in Figs. 2, 3, for  $a > 4 \mu\text{m}$  the results in both models coincide with one another and for separations  $a > 6 \mu\text{m}$  coincide also with the case of ideal metal.

Now let us derive some analytic results for the configuration of two plane parallel plates using both the plasma and Drude models. In the plasma model it is possible to obtain the perturbation expansion of Eq. (23) in terms of a small parameter  $\delta_0/a$ , where  $\delta_0 = c/\omega_p$  is the effective penetration depth of the electromagnetic zero-point oscillations into the metal. For this purpose it is useful to introduce the new variable  $v = \tilde{\xi}/y$  instead of  $\tilde{\xi}$  and to rewrite Eq. (23) in the form

$$F_{ss}(a) = -\frac{\hbar c}{16\pi^2 a^4} \sum_{l=0}^{\infty} \int_0^{\infty} y^3 dy \int_0^1 dv \cos(lvyt) f_{ss}(v, y). \quad (52)$$

Expanding the quantity  $f_{ss}$  defined in (20) up to the first order in powers of  $\delta_0/a$  one obtains

$$f_{ss}(v, y) = \frac{2}{e^y - 1} - 2 \frac{ye^y}{(e^y - 1)^2} (1 + v^2) \frac{\delta_0}{a}. \quad (53)$$

Substituting Eq. (53) into Eq. (52) we come after some transformations to the Casimir force including the effect of both the nonzero temperature and finite conductivity

$$\begin{aligned} F_{ss}(a) = F_{ss}^0(a) & \left\{ 1 + \frac{30}{\pi^4} \sum_{l=1}^{\infty} \left[ \frac{1}{t^4 l^4} - \frac{\pi^3}{tl} \frac{\cosh(\pi tl)}{\sinh^3(\pi tl)} \right] \right. \\ & - \frac{16}{3} \frac{\delta_0}{a} - 60 \frac{\delta_0}{a} \sum_{l=1}^{\infty} \left[ \frac{2\cosh^2(\pi tl) + 1}{\sinh^4(\pi tl)} - \frac{2\cosh(\pi tl)}{\pi tl \sinh^3(\pi tl)} \right. \\ & \left. \left. - \frac{1}{2\pi^2 t^2 l^2 \sinh^2(\pi tl)} - \frac{\coth(\pi tl)}{2\pi^3 t^3 l^3} \right] \right\}, \end{aligned} \quad (54)$$

where  $F_{ss}^0(a) = F_{ss}^0(a, 0) \equiv -\pi^2 \hbar c / (240a^4)$  is the zero-temperature Casimir force between ideal metals. The first summation in (54) is exactly the temperature correction in the case of ideal metals (see, e.g., [18]). The second summation takes into account the effect of finite conductivity combined with nonzero temperature.

In the limit of low temperatures  $T \ll T_{eff}$  one has from (54) neglecting terms exponentially small in  $2\pi T_{eff}/T$  [33]

$$F_{ss}(a) \approx F_{ss}^0(a) \left\{ 1 + \frac{1}{3} \left( \frac{T}{T_{eff}} \right)^4 - \frac{16}{3} \frac{\delta_0}{a} \left[ 1 - \frac{45\zeta(3)}{8\pi^3} \left( \frac{T}{T_{eff}} \right)^3 \right] \right\}. \quad (55)$$

For  $\delta_0 = 0$  (perfect conductor) Eq. (55) turns into the well known result [18] demonstrating that the first nonzero temperature correction is of the fourth power in  $T/T_{eff}$ . For  $T = 0$  the first-order finite conductivity correction to the Casimir force [17, 18] is reproduced from (55). Note that the first correction of mixing finite conductivity and finite temperature is of order  $(T/T_{eff})^3$ . More significantly, note that there are no temperature corrections of order  $(T/T_{eff})^k$  with  $k \leq 4$  in the higher order conductivity correction terms  $(\delta_0/a)^i$  from the second up to the sixth order [33].

In the Drude model the analytical results can be obtained in the high-temperature limit  $T \gg T_{eff}$ . It is easily seen that at high temperatures (large separations) only one term of Eq. (35) with  $l = 0$  contributes the result, the other terms with  $l \geq 1$  being exponentially small in the parameter  $2\pi T/T_{eff}$ . The situation here is exactly the same as for the ideal metal [18]. As a consequence, Eq. (35) can be rewritten in the following form

$$F_{ss}(a) = -\frac{k_B T}{16\pi a^3} \left[ \int_0^\infty \frac{y^2 dy}{e^y - 1} + \int_0^\infty \frac{y^2 dy}{r_2^{-2}(y, y) e^y - 1} \right]. \quad (56)$$

It is seen from Eq. (56) that in the high-temperature limit only the perpendicular reflection coefficient  $r_2$  gives rise to the finite conductivity corrections to the Casimir force (the same is valid in plasma model also).

After the straightforward calculations up to the first orders in small parameters  $\delta_0/a$ ,  $\gamma/\omega_p$  (see the details in Appendix II) the result

$$F_{ss}(a) = F_{ss}^0(a, T) \left[ 1 - 3 \frac{\delta_0}{a} - \frac{\gamma}{\omega_p} \frac{1}{\zeta(3)} I_1(\tilde{\gamma}) \right] \quad (57)$$

is obtained, where  $I_1$  is a function slowly depending on the effective relaxation parameter (space separation) and given by

$$I_1(\tilde{\gamma}) = \int_0^\infty dy \frac{y^2 \sqrt{y}}{\sqrt{y + \tilde{\gamma} + \sqrt{y}}} \frac{e^y}{(e^y - 1)^2}. \quad (58)$$

At high temperatures, which are considered here, the Casimir force acting between the ideal metals is

$$F_{ss}^0(a, T) = -\frac{k_B T}{4\pi a^3} \zeta(3), \quad (59)$$

where  $\zeta(3) \approx 1.202$  is the Riemann zeta function.

With the above value of relaxation frequency for *Al* one has  $I_1 \approx 1.16$  at  $a = 5 \mu\text{m}$  and  $I_1 \approx 0.99$  at  $a = 10 \mu\text{m}$ . In Appendix II (Fig. 8) the functional dependence of  $I_1$  on  $\tilde{\gamma}$  is plotted. As is seen from (57), the high-temperature Casimir force depends on both plasma frequency and relaxation frequency. For all  $a > 6 \mu\text{m}$  the results obtained by the asymptotic Eq. (57) coincide with the above results of numerical computations (see Figs. 2 and 3). The characteristic size of the conductivity correction at large separations can be estimated from the following example. At  $a = 10 \mu\text{m}$  the finite conductivity correction obtained from (57) is  $\delta_c(F_{ss}^D) \approx 0.89\%$  and with  $\gamma = 0$  it holds  $\delta_c(F_{ss}^p) \approx 0.47\%$  in perfect agreement with Figs. 2, 3. The smooth joining of the results obtained using the Drude model with those using the plasma model when  $\gamma \rightarrow 0$  is evident.

Note that in the framework of the approach used in [34, 35] the high temperature Casimir force between real metals is given by  $F_{ss}(a) = F_{ss}^0(a, T)/2$  (see Eq. (59)), i.e. two times smaller than for ideal metal, regardless of the conductivity properties of a real metal used. As to the approach used in [36, 37], the asymptotic behavior at high temperatures coincides with

Eq. (59), i.e. it is the same as the case for ideal metals in both plasma and Drude models. Once again, the real properties of a metal do not influence the result.

## V COMPUTATIONS OF THE CASIMIR FORCE BETWEEN A PLATE AND A SPHERICAL LENS MADE OF REAL METAL

The configuration of a spherical lens (or a sphere) above a semispace (plate) was found to be the most suitable for the precision measurements of the Casimir force [7, 8, 9, 10, 11, 12]. In these experiments the finite conductivity corrections have been demonstrated [8, 9, 10, 11, 12] and the sensitivity for the detection of the temperature corrections is close to being achieved [7]. For this reason the combined effect of both corrections is of extreme interest. Here the computations of the Casimir force for the configuration of a lens above a plate are performed using the Drude and plasma models with parameters of Eq. (49). The results obtained by our Eq. (48) are compared with the computations of other authors.

We start with the relative temperature correction

$$\delta_T(F_{sl}^f) = \frac{F_{sl}^f(a, T_0) - F_{sl}^f(a, 0)}{F_{sl}^f(a, 0)}, \quad (60)$$

where all the notations and parameters are the same as in Eq. (50) and only the configuration is different. The results of numerical computations by Eqs. (48), (60) in the case of Drude model are presented in Fig. 5 by the solid curve 1. The solid curve 2 represents the temperature correction in the case of a dielectric plate and a lens (see the next section). By the dashed curve the results obtained by the approach of [34, 35] are shown. The curve 1 increases monotonically in perfect analogy with Fig. 1. However, the dashed curve represents the negative temperature correction at separations  $a \leq 4.1 \mu\text{m}$  and changes sign for larger separations. This behavior corresponds to the case

where large by modulus corrections linear in temperature to the ideal zero-temperature Casimir force are present. According to [38] such corrections are in contradiction with the experimental data of [7]. On the basis of our Eq. (48) such corrections do not arise.

In Table 2 the values of the relative temperature corrections are presented at different distances between a lens and a plate computed using the Drude model (present paper, column 2) and the plasma model (present paper, column 3), the ideal metal (column 4), computed on the basis of [35] using the Drude model (column 5), and on the basis of [36, 37] using Drude and plasma models (columns 6 and 7 respectively).

From Table 2 (columns 2–4) it follows that at smallest separations the temperature correction computed using the Drude model is about two orders of magnitude larger than with the plasma model and for the ideal metal. At large separations the predictions of both models are very close to each other and to the results obtained with the ideal metal (column 4). The negative and large magnitude of the corrections at small separations results of column 5, computed on the basis of [35], correspond to linear temperature corrections. The results of columns 6, 7, although positive, also correspond to the presence of linear temperature corrections at small separations.

The relative finite conductivity correction at a temperature  $T_0$  can be described by

$$\delta_c(F_{sl}^f) = \frac{F_{sl}^0(a, T_0) - F_{sl}^f(a, T_0)}{F_{sl}^0(a, T_0)}. \quad (61)$$

In Fig. 6 this quantity is plotted as a function of separation in the case of the Drude model at  $T_0 = 300$  K (solid curve is our result computed by Eq. (48), the long-dashed curve is computed on the basis of [36, 37]). The dependence of the conductivity correction on separation at  $T_0 = 0$  is shown by the short-dashed curve. In Fig. 7 the analogous results computed using the plasma model are presented. As with the case of two plane plates (Sec. IV), Drude model leads to larger finite conductivity corrections than the plasma model. At separations larger than  $4 \mu\text{m}$  the conductivity correction computed using

[36, 37] turns into zero with both Drude and plasma models (the long-dashed curves in Figs. 6, 7). Once more, this property is determined by the artificial modification of the zeroth term of Lifshitz formula used in [36, 37] and does not depend on the particular characteristics of a real metal.

In the same way as for two plane plates our results for a lens above a plate, computed using the Drude model, join smoothly when  $\gamma \rightarrow 0$  with the results computed with the plasma model. This is not the case in the approach of [34, 35].

We come now to the perturbative analytical results which can be obtained for the configuration of a lens above a plate. Here, the plasma model can be used. Introducing the new variable  $v = \tilde{\xi}/y$  instead of  $\tilde{\xi}$  one obtains

$$F_{sl}(a) = \frac{\hbar c R}{8\pi a^3} \sum_{l=0}^{\infty} \int_0^{\infty} y^2 dy \int_0^1 dv \cos(ltv y) f_{sl}(v, y). \quad (62)$$

The expansion of  $f_{sl}$  up to first order in the small parameter  $\delta_0/a$  is

$$f_{sl}(v, y) = 2 \ln(1 - e^{-y}) + 2 \frac{y}{e^y - 1} (1 + v^2) \frac{\delta_0}{a}. \quad (63)$$

Substitution of Eq. (63) into Eq. (60) leads to result

$$F_{sl}(a) = F_{sl}^0(a) \left\{ 1 + \frac{45}{\pi^3} \sum_{l=1}^{\infty} \left[ \frac{\coth(\pi tl)}{t^3 l^3} + \frac{\pi}{t^2 l^2 \sinh^2(\pi tl)} \right] - \frac{1}{t^4} \right. \\ \left. - 4 \frac{\delta_0}{a} + \frac{180}{\pi^4} \frac{\delta_0}{a} \sum_{l=1}^{\infty} \left[ \frac{\pi \coth(\pi tl)}{2t^3 l^3} - \frac{2}{t^4 l^4} + \frac{\pi^3 \coth(\pi tl)}{t l \sinh^2(\pi tl)} \right. \right. \\ \left. \left. + \frac{\pi^2}{t^2 l^2 \sinh^2(\pi tl)} \right] \right\}, \quad (64)$$

where  $F_{sl}^0(a) = F_{sl}^0(a, 0) \equiv -\pi^3 \hbar c R / (360 a^3)$ .

For the case of low temperatures  $T \ll T_{eff}$  Eq. (64) leads to [33]

$$F_{sl}(a) \approx F_{sl}^0(a) \left\{ 1 + \frac{45\zeta(3)}{\pi^3} \left( \frac{T}{T_{eff}} \right)^3 - \left( \frac{T}{T_{eff}} \right)^4 \right. \\ \left. - 4 \frac{\delta_0}{a} \left[ 1 - \frac{45\zeta(3)}{2\pi^3} \left( \frac{T}{T_{eff}} \right)^3 + \left( \frac{T}{T_{eff}} \right)^4 \right] \right\}. \quad (65)$$

The corrections to (65) are exponentially small in the parameter  $2\pi T_{eff}/T$ . For ideal metal  $\delta_0 = 0$  and Eq. (65) coincides with the known result [7]. It is seen that for the perfectly conducting lens and plate the first nonzero temperature correction is of the third order in  $T/T_{eff}$ . For  $T = 0$  the first order finite conductivity correction to the Casimir force [20] is reproduced. In analogy with two plane plates the perturbation orders  $(\delta_0/a)^i$  with  $2 \leq i \leq 6$  do not contain temperature corrections of orders  $(T/T_{eff})^3$  and  $(T/T_{eff})^4$  or smaller ones [33].

Now we consider the analytical results which can be obtained with the Drude model at high temperature  $T \gg T_{eff}$ . Here only the zeroth term of Lifshitz formula contributes the result. Then Eq. (48) can be represented as

$$F_{sl}(a) = \frac{k_B T R}{8a^2} \left\{ \int_0^\infty y dy \ln(1 - e^{-y}) + \int_0^\infty y dy \ln[1 - r_2^2(y, y)e^{-y}] \right\}. \quad (66)$$

After some transformations (see Appendix II) one arrives at the result

$$F_{sl}(a) = F_{sl}^0(a, T) \left[ 1 - 2\frac{\delta_0}{a} - \frac{\gamma}{\omega_p} \frac{2}{\zeta(3)} I_2(\tilde{\gamma}) \right], \quad (67)$$

where  $I_2$  is defined by

$$I_2(\tilde{\gamma}) = \int_0^\infty dy \frac{y\sqrt{y}}{\sqrt{y + \tilde{\gamma}} + \sqrt{y}} \frac{1}{e^y - 1}. \quad (68)$$

The high-temperature Casimir force acting between the lens and the plate made of ideal metal is

$$F_{sl}^0(a, T) = -\frac{k_B T R}{4a^2} \zeta(3). \quad (69)$$

For example,  $I_2 \approx 0.519$  at  $a = 5 \mu\text{m}$  and  $I_1 \approx 0.434$  at  $a = 10 \mu\text{m}$  (using the data of (49) for  $Al$ ). The dependence of  $I_2$  on  $\tilde{\gamma}$  is plotted in Appendix II (Fig. 8). The asymptotic results of Eq. (67) coincide with the results of numerical computations for  $a > 5 \mu\text{m}$ . The choice of the model describing dielectric properties of a metal at large separations is rather important. At  $a = 10 \mu\text{m}$  the conductivity correction is  $\delta_c(F_{sl}^D) \approx 0.68\%$  using the Drude

model and  $\delta_c(F_{sl}^p) \approx 0.32\%$  using plasma model, i.e. more than two times smaller. In analogy with two plates, the high-temperature Casimir force calculated on the basis of [35] is two times smaller than in (69) regardless of the conductivity properties of the metal. In [36, 37] the high-temperature behavior for the real metals coincides with (69) obtained for the ideal metal. So, the actual properties of a particular metal are not reflected.

## VI TEMPERATURE CASIMIR FORCE BETWEEN THE DIELECTRIC TEST BODIES

Here we briefly discuss the temperature Casimir force between dielectrics. The application of Lifshitz formulas (1) or (37) for the case of dielectric surfaces is direct. No additional prescriptions, such as the ones used above or their generalizations are needed to obtain the final result matching the general physical requirements. However, when the formalism developed for dielectrics is compared with that for metals, the origin of the above difficulties becomes clear.

The dielectric permittivity of dielectrics can be modeled, e.g., by the Mahanty-Ninham relation [46, 54]

$$\varepsilon(i\xi) = 1 + \frac{\varepsilon_0 - 1}{1 + \frac{\xi^2}{\omega_e^2}}. \quad (70)$$

Here  $\omega_e \sim 2 \times 10^{16}$  Hz gives the main electronic absorption in the ultraviolet,  $\varepsilon_0$  is the static dielectric constant. At small  $\xi \ll \omega_e$  one has  $\varepsilon(i\xi) \approx \varepsilon_0$ . In fact, frequencies giving large contributions to the Lifshitz formulas (1) or (37) in the micrometer separation range are much smaller than  $\omega_e$ . Because of this,  $\varepsilon(i\xi)$  can be approximately replaced by  $\varepsilon_0$ . Below we use in all computations  $\varepsilon_0 \approx 7$  which corresponds to the sheet of mica.

In reality, the zeroth term of Lifshitz formula for dielectrics is also discontinuous as in the case of metals. To illustrate this statement we put  $l = 0$  in (3) and obtain the following values of the reflection coefficients defined in

Eq. (2)

$$r_1^2(0, k_{\perp}) = \left( \frac{\varepsilon_0 - 1}{\varepsilon_0 + 1} \right)^2, \quad r_2^2(0, k_{\perp}) = 0. \quad (71)$$

These values do not depend on  $k_{\perp}$ . Therefore they are preserved in the limit  $k_{\perp} \rightarrow 0$ . At the same time, if we put  $k_{\perp} = 0$  from the very beginning one obtains

$$r_1^2(\xi_l, 0) = r_2^2(\xi_l, 0) = r^{(R)} \equiv \left( \frac{\sqrt{\varepsilon_0} - 1}{\sqrt{\varepsilon_0} + 1} \right)^2, \quad (72)$$

which is the case for real photons. These values do not depend on  $\xi_l$  and are preserved in the limit  $\xi_l \rightarrow 0$ . Eqs. (71), (72) together imply that both reflection coefficients  $r_1(\xi, k_{\perp})$  and  $r_2(\xi, k_{\perp})$  are discontinuous as the functions of two variables at a point (0,0). Remind that in the case of metals described by Drude model only the transverse reflection coefficient  $r_2$  was discontinuous (see Sec. II). Note that in the zeroth term of the Lifshitz formula for dielectrics both reflection coefficients (71) correspond to nonphysical (virtual) photons with  $r_1 > r^{(R)}$  and  $r_2 < r^{(R)}$ . At the same time, for metals the longitudinal reflection coefficient at zero frequency takes the physical value  $r_1 = r^{(R)} = 1$  in both plasma and Drude models. As to the perpendicular reflection coefficient at zero frequency in the case of metals, it corresponds to nonphysical photons and takes the values  $r_2 = 0 < r^{(R)} = 1$  in Drude model and  $r_2 = g(k_{\perp}) < r^{(R)} = 1$  in the plasma model (see Eqs. (13), (15)).

It is of paramount importance that the discontinuity of both reflection coefficients causes no physical problem in the cases of dielectrics. The point is that the dielectric permittivity (70) corresponds to a nondissipative medium (which is not the case for metals described by the Drude model). For this reason, the scattering problem, which underlies the Lifshitz theory (see Sec. II and also [48]), is well defined at zero frequency through the unitarity of scattering matrix, furnishing the desired value of the scattering coefficient and thereby the free energy. The results obtained for dielectrics are physically consistent. They are immediately evident from Eqs. (1), (37) without use of any additional assumptions which are necessary in both cases of ideal and real metals where the scattering problem at zero frequency is not well defined.

The results of numerical computations for the dielectric test bodies made of mica are shown by the solid curves 2 in Fig. 1 (Eq. (1), two plane plates) and in Fig. 5 (Eq. (37), a lens above a plate). The curve 2 is in direct analogy with the curve 1 in the same figure. At all separations the relative temperature correction for dielectrics is positive. At  $a = 0.1 \mu\text{m}$  it takes the value  $\delta_T(F_{ss}) = 1.94 \times 10^{-5}$ . This is larger than for ideal metal and for real metal (*Al*) considered in framework of the plasma model but smaller than for the same metal in framework of the Drude model (see Table I). At  $a = 1 \mu\text{m}$  and  $a = 10 \mu\text{m}$  there are  $\delta_T(F_{ss}) = 1.99 \times 10^{-2}$ , respectively,  $\delta_T(F_{ss}) = 2.50$  for dielectrics. At  $a \geq 1 \mu\text{m}$  the temperature correction for dielectrics is larger than for ideal or real metals at the same separation. For the configuration of a dielectric lens above a disk at separations  $a = 0.1, 1$  and  $10 \mu\text{m}$  the temperature correction is, respectively,  $2.39 \times 10^{-4}$ ,  $6.94 \times 10^{-2}$ , and 4.25. The relationship of these values with those computed for the real and ideal metals (see Table II) is the same as in the case of two plane plates.

## VII CONCLUSIONS AND DISCUSSION

As demonstrated above, the computation of the Casimir force between real metals at nonzero temperature is a complicated theoretical problem. The first contradictions between Lifshitz theory [2, 16] applied to ideal metals and calculations based on quantum field theory [28, 29] were revealed in the sixties. They were resolved by Schwinger, DeRaad and Milton [18] by the use of special prescription modifying the zero-frequency term of Lifshitz formula. After the use of this prescription the results of [2, 16] in application to ideal metal became agreed with those of [28, 29].

A new stage in the solution of the problem has been started only recently. It was motivated by the increased accuracy of the Casimir force measurements and possible applications of the Casimir effect as a test of fundamental physical theories and in nanotechnology. Different authors [32, 33, 34, 35, 36, 37] applied Lifshitz theory to calculate the temperature Casimir force between

real metals and obtained the diverse results. In [34, 35] the Lifshitz formula was applied to real metals in its original form without any modification of the zero-frequency term. The obtained results, however, turned out to be in contradiction with experiment (see Sec. V) and with general theoretical requirements (negative temperature corrections at small distances and incorrect asymptotic at high temperatures, see Secs. II, IV, V). In [36, 37] the zeroth term of Lifshitz formula for real metals at nonzero temperature was modified according to the prescription of [18] formulated for ideal metals. The obtained results were compared with the Casimir force at zero temperature which was computed for real metals without use of any prescription. Such an approach leads to significant temperature corrections to the Casimir force at small separations (both in plasma and Drude models) which are linear in temperature and also to the absence of any finite conductivity corrections at the moderate separations. In [32, 33] the computations of the temperature Casimir force in frames of plasma model were performed with the coinciding results (no linear in temperature corrections were found at small distances). These computations did not use any modification of Lifshitz formula. In [33] the problems arising in frames of Drude model were also formulated and the way to their solution was directed.

In the present paper we propose the new prescription modifying the zeroth term of Lifshitz formula in the case of real metals described by Drude model (Secs. II, III). The necessity of this prescription has in-depth reasons connected with the failure of scattering formalism underlying Lifshitz formula in the case when the dielectric permittivity describes a medium with dissipation where the unitarity condition is absent. This prescription is the generalization of the Schwinger, DeRaad and Milton prescription [18] for the case of real metal. In the case of plasma model (which describes a nondissipative medium) it leads to exactly the same results as an unmodified Lifshitz formula. Because of this all the results obtained in [32, 33] preserve their validity.

The Lifshitz formula with the modified zero-frequency term is given by Eq. (35) (configuration of two plane plates) and by Eq. (48) (configuration of a lens above a plate). The detailed computations with the use of these equations were performed in Secs. IV, V. It was shown that the obtained temperature corrections are positive and offer the correct asymptotic behavior both at small and high temperatures (separations). The results obtained in frames of Drude model join smoothly with those obtained in frames of plasma model when the relaxation frequency goes to zero. The finite conductivity corrections to the Casimir force were computed at nonzero temperature in the separation range from  $0.1\text{ }\mu\text{m}$  till  $10\text{ }\mu\text{m}$  in frames of Drude and plasma models. Both the temperature and finite conductivity corrections calculated above possess the reasonable physical properties avoiding difficulties which arise in [34, 35] and in [36, 37]. The perturbative analytical results at both small and large separations are in agreement with the numerical computations. The case of dielectric test bodies (Sec. VI) where the scattering problem is consistent at all frequencies illustrates the essence of difficulties arising in the case of real metals.

In the nearest future one should expect the experimental registration of the temperature Casimir force. This will be the final answer in the discussion on the subject what is the temperature dependence of the Casimir force. Meanwhile it is necessary to proceed with the more detailed elaboration of the microscopic theory of dispersion forces based on quantum field theory at nonzero temperature in Matsubara formulation. There is a real possibility that the above phenomenological prescription, concerning the zero-frequency contribution to Lifshitz formula, will be rigorously derived, at least as a good approximation, in terms of the scattering theory in dissipative media. The final solution of this problem seems to be of large importance taking into account the prospective role of dispersion forces in both fundamental and applied science.

## ACKNOWLEDGMENTS

The authors are grateful for helpful discussions to M.Bordag, I.A. Merkulov, U. Mohideen, and V.I. Perel'. They are indebted to the Brazilian Center of Physical Research (Rio de Janeiro) and Physics Department of the Federal University of Paraíba (João Pessoa) for kind hospitality. This work was partially supported by FAPERJ and CNPq.

## APPENDIX I

In this Appendix Eqs. (26), (27) are derived starting from Eq. (25). Using (20), Eq. (25) can be rewritten in the form

$$\begin{aligned}
F_{ss}(a) = & -\frac{\hbar c}{32\pi^2 a^4} \int_0^\infty y^2 dy \left\{ \frac{1}{2} \int_0^y d\tilde{\xi} f_{ss}(\tilde{\xi}, y) \right. \\
& + \frac{\pi}{2t} \left[ f_{ss}^{(1)}(y, y) - \int_0^y d\tilde{\xi} \frac{\partial f_{ss}^{(1)}(\tilde{\xi}, y)}{\partial \tilde{\xi}} \right] \\
& + \frac{\pi}{2t} \left[ f_{ss}^{(2)}(y, y) - \int_0^y d\tilde{\xi} \frac{\partial f_{ss}^{(2)}(\tilde{\xi}, y)}{\partial \tilde{\xi}} \right] \\
& - \frac{1}{2} y f_{ss}(y, y) \\
& + \frac{1}{2} \left[ \tilde{\xi} f_{ss}(\tilde{\xi}, y) \Big|_0^y - \int_0^y d\tilde{\xi} f_{ss}(\tilde{\xi}, y) \right] \\
& + \frac{\pi}{t} f_{ss}(y, y) A\left(\frac{ty}{2\pi}\right) \\
& \left. - \frac{\pi}{t} \int_0^y d\tilde{\xi} \frac{\partial f_{ss}(\tilde{\xi}, y)}{\partial \tilde{\xi}} A\left(\frac{t\tilde{\xi}}{2\pi}\right) \right\}. \tag{I.1}
\end{aligned}$$

The functions  $f_{ss}^{(1)}$  and  $\partial f_{ss}^{(1)}/\partial \tilde{\xi}$  are continuous at all points for both plasma and Drude models. Due to this it holds

$$\int_0^y d\tilde{\xi} \frac{\partial f_{ss}^{(1)}(\tilde{\xi}, y)}{\partial \tilde{\xi}} = f_{ss}^{(1)}(y, y) - f_{ss}^{(1)}(0, y). \tag{I.2}$$

Note that the same equality is not valid for  $f_{ss}^{(2)}$  because it is discontinuous at zero frequency. Substituting (I.2) into (I.1) and performing the cancellations

one obtains

$$\begin{aligned}
F_{ss}(a) = & -\frac{\hbar c}{16\pi^2 a^4} \int_0^\infty y^2 dy \left\{ \frac{\pi}{2t} [f_{ss}^{(1)}(0, y) + f_{ss}^{(2)}(y, y)] \right. \\
& - \frac{\pi}{2t} \int_0^y d\tilde{\xi} \frac{\partial f_{ss}^{(2)}(\tilde{\xi}, y)}{\partial \tilde{\xi}} \\
& + \frac{\pi}{t} f_{ss}(y, y) A\left(\frac{ty}{2\pi}\right) \\
& \left. - \frac{\pi}{t} \int_0^y d\tilde{\xi} \frac{\partial f_{ss}(\tilde{\xi}, y)}{\partial \tilde{\xi}} A\left(\frac{t\tilde{\xi}}{2\pi}\right) \right\}. \tag{I.3}
\end{aligned}$$

Now let us consider two last contributions to (I.3) containing the function  $A(z)$ . With account of Eq. (19)  $\tau = 2\pi T/T_{eff} = 2\pi/t$ . According to definition of the integer portion function

$$A\left(\frac{ty}{2\pi}\right) = A\left(\frac{y}{\tau}\right) = k \text{ if } k\tau \leq y < (k+1)\tau \tag{I.4}$$

for  $k = 0, 1, 2, \dots$ . Using (I.4) the integral from (I.3) can be represented as

$$\begin{aligned}
\int_0^\infty y^2 dy f_{ss}(y, y) A\left(\frac{ty}{2\pi}\right) &= \int_\tau^{2\tau} y^2 dy f_{ss}(y, y) \\
&+ 2 \int_{2\tau}^{3\tau} y^2 dy f_{ss}(y, y) + \dots + l \int_{l\tau}^{(l+1)\tau} y^2 dy f_{ss}(y, y) + \dots \\
&= \int_\tau^\infty y^2 dy f_{ss}(y, y) + \int_{2\tau}^\infty y^2 dy f_{ss}(y, y) + \dots + \int_{l\tau}^\infty y^2 dy f_{ss}(y, y) + \dots \\
&= \sum_{l=1}^{\infty} \int_{l\tau}^\infty y^2 dy f_{ss}(y, y). \tag{I.5}
\end{aligned}$$

The second integral from (I.3) containing the integer portion function is a bit more complicated. Using the definition of this function, it can be represented in the following form

$$\begin{aligned}
\int_0^\infty y^2 dy \int_0^y d\tilde{\xi} \frac{\partial f_{ss}(\tilde{\xi}, y)}{\partial \tilde{\xi}} A\left(\frac{t\tilde{\xi}}{2\pi}\right) &= \int_\tau^{2\tau} y^2 dy \int_\tau^y d\tilde{\xi} \frac{\partial f_{ss}(\tilde{\xi}, y)}{\partial \tilde{\xi}} \\
&+ \int_{2\tau}^{3\tau} y^2 dy \left[ \int_\tau^{2\tau} d\tilde{\xi} \frac{\partial f_{ss}(\tilde{\xi}, y)}{\partial \tilde{\xi}} + 2 \int_{2\tau}^y d\tilde{\xi} \frac{\partial f_{ss}(\tilde{\xi}, y)}{\partial \tilde{\xi}} \right] + \dots
\end{aligned}$$

$$\begin{aligned}
& + \int_{l\tau}^{(l+1)\tau} y^2 dy \left[ \int_{\tau}^{2\tau} d\tilde{\xi} \frac{\partial f_{ss}(\tilde{\xi}, y)}{\partial \tilde{\xi}} + 2 \int_{2\tau}^{3\tau} d\tilde{\xi} \frac{\partial f_{ss}(\tilde{\xi}, y)}{\partial \tilde{\xi}} + \dots \right. \\
& \left. + l \int_{l\tau}^y d\tilde{\xi} \frac{\partial f_{ss}(\tilde{\xi}, y)}{\partial \tilde{\xi}} \right] + \dots . \tag{I.6}
\end{aligned}$$

Now we calculate all integrals with respect to  $\tilde{\xi}$  according to

$$\int_a^b d\tilde{\xi} \frac{\partial f_{ss}(\tilde{\xi}, y)}{\partial \tilde{\xi}} = f_{ss}(b, y) - f_{ss}(a, y). \tag{I.7}$$

For all  $a \neq 0$ , as it is in (I.6), Eq. (I.7) is valid for both polarizations (i.e. for both  $f_{ss}^{(1)}$  and  $f_{ss}^{(2)}$ ) because the quantities under consideration are continuous. The result is

$$\begin{aligned}
& \int_0^\infty y^2 dy \int_0^y d\tilde{\xi} \frac{\partial f_{ss}(\tilde{\xi}, y)}{\partial \tilde{\xi}} A \left( \frac{t\tilde{\xi}}{2\pi} \right) = \int_{\tau}^{2\tau} y^2 dy [f_{ss}(y, y) - f_{ss}(\tau, y)] \\
& + \int_{2\tau}^{3\tau} y^2 dy [2f_{ss}(y, y) - f_{ss}(\tau, y) - f_{ss}(2\tau, y)] + \dots \\
& + \int_{l\tau}^{(l+1)\tau} y^2 dy [lf_{ss}(y, y) - f_{ss}(\tau, y) - f_{ss}(2\tau, y) - \dots - f_{ss}(l\tau, y)] + \dots . \tag{I.8}
\end{aligned}$$

Combining the terms with identical arguments and using (I.5), we obtain

$$\begin{aligned}
& \int_0^\infty y^2 dy \int_0^y d\tilde{\xi} \frac{\partial f_{ss}(\tilde{\xi}, y)}{\partial \tilde{\xi}} A \left( \frac{t\tilde{\xi}}{2\pi} \right) = - \sum_{l=1}^{\infty} \int_{l\tau}^{\infty} y^2 dy f_{ss}(l\tau, y) \\
& + \sum_{l=1}^{\infty} \int_{l\tau}^{\infty} y^2 dy f_{ss}(y, y). \tag{I.9}
\end{aligned}$$

Now we substitute (I.5) and (I.9) into (I.3) with the result

$$\begin{aligned}
F_{ss}(a) = & - \frac{\hbar c}{32\pi a^4 t} \int_0^\infty y^2 dy \left[ f_{ss}^{(1)}(0, y) + f_{ss}^{(2)}(y, y) \right. \\
& \left. - \int_0^y d\tilde{\xi} \frac{\partial f_{ss}^{(2)}(\tilde{\xi}, y)}{\partial \tilde{\xi}} \right] - \frac{\hbar c}{16\pi a^4 t} \sum_{l=1}^{\infty} \int_{l\tau}^{\infty} y^2 dy f_{ss}(l\tau, y). \tag{I.10}
\end{aligned}$$

With account of  $t \equiv T_{eff}/T = \hbar c/(2ak_B T)$  and  $l\tau \equiv \tilde{\xi}_l$  Eq. (I.10) coincides with Eqs. (26), (27).

## APPENDIX II

In this Appendix Eqs. (57), (67) are obtained and the integral quantities  $I_n(\tilde{\gamma})$  ( $i = 1, 2$ ) are computed. The expression under the second integral in the right-hand side of Eq. (56) is approximately equal to

$$\frac{y^2}{r_2^{-2}e^y - 1} \approx \frac{y^2}{e^y - 1} - 2\frac{\delta_0}{a}y^2\sqrt{y(y + \tilde{\gamma})}\frac{e^y}{(e^y - 1)^2}, \quad (\text{II.1})$$

where the terms up to the first order in small parameter  $\delta_0/a$  are preserved. Notice that the first contribution here is the same as under the first integral in (56). They together produce the high-temperature asymptotic for the case of ideal metal. The second contribution in (II.1) takes the effects of finite conductivity into account. This second contribution can be identically represented as

$$-2\frac{\delta_0}{a}y^2\sqrt{y(y + \tilde{\gamma})}\frac{e^y}{(e^y - 1)^2} = -2\frac{\delta_0}{a}\left[\frac{y^3e^y}{(e^y - 1)^2} + \tilde{\gamma}\frac{y^2\sqrt{y}}{\sqrt{y + \tilde{\gamma}} + \sqrt{y}}\frac{e^y}{(e^y - 1)^2}\right]. \quad (\text{II.2})$$

Substituting (II.1), (II.2) with account of  $2\delta_0/a = 4/\tilde{\omega}_p$  and  $\tilde{\gamma}/\tilde{\omega}_p \equiv \gamma/\omega_p$  into (56) one obtains

$$F_{ss}(a) = -\frac{k_B T}{16\pi a^3} \left[ 4\zeta(3) - 12\zeta(3)\frac{\delta_0}{a} - 4\frac{\gamma}{\omega_p} I_1(\tilde{\gamma}) \right], \quad (\text{II.3})$$

where  $I_1(\tilde{\gamma})$  was defined in (58). This equation coincides with Eq. (57) because of (59).

In Fig. 8 the dependence of  $I_1$  on  $\tilde{\gamma}$  is plotted (curve 1). The values of  $I_1$  decrease from 1.3844 at  $\tilde{\gamma} = 1$  until 0.8782 at  $\tilde{\gamma} = 10$ . With account of definition of Sec. II  $\tilde{\gamma} = 2a\gamma/c$  the dependence of  $I_1$  on  $\tilde{\gamma}$  may be recalculated into the dependence of  $I_1$  on  $a$  at fixed  $\gamma$ . To take an example, with the above value of  $\gamma = 9.6 \times 10^{13}$  rad/s  $\tilde{\gamma}$  changes in the interval  $1.92 \leq \tilde{\gamma} \leq 6.4$  when the separation distance belongs to the interval  $3 \mu\text{m} \leq a \leq 10 \mu\text{m}$ .

We now turn to the derivation of Eq. (67). The expression under the second integral in the right-hand side of Eq. (66) calculated up to the first

order in  $\delta_0/a$  is

$$y \ln [1 - r_2^2(y, y)e^{-y}] \approx y \ln(1 - e^{-y}) + 2 \frac{\delta_0}{a} \sqrt{y(y + \tilde{\gamma})} \frac{y}{e^y - 1}. \quad (\text{II.4})$$

Once more the first contribution here is the same as under the first integral in (66). Together they produce the high-temperature Casimir force between a lens and a plate made of ideal metal. The second contribution in (II.4) is responsible for the finite conductivity correction. This second contribution can be rewritten in the form

$$2 \frac{\delta_0}{a} \sqrt{y(y + \tilde{\gamma})} \frac{y}{e^y - 1} = 2 \frac{\delta_0}{a} \left( \frac{y^2}{e^y - 1} + \tilde{\gamma} \frac{y\sqrt{y}}{\sqrt{y + \tilde{\gamma}} + \sqrt{y}} \frac{1}{e^y - 1} \right). \quad (\text{II.5})$$

Substituting (II.4) and (II.5) into Eq. (66) and performing the integration one obtains

$$F_{sl}(a) = \frac{k_B T R}{8a^2} \left[ -2\zeta(3) + 4\zeta(3) \frac{\delta_0}{a} + 4 \frac{\gamma}{\omega_p} I_2(\tilde{\gamma}) \right], \quad (\text{II.6})$$

where  $I_2(\tilde{\gamma})$  was defined in (68). Eq. (II.6) coincides with Eq. (67) if to take account of (69).

In Fig. 8 the dependence of  $I_2$  on  $\tilde{\gamma}$  is shown by the curve 2. The values of  $I_2$  decrease from 0.6455 at  $\tilde{\gamma} = 1$  until 0.3787 at  $\tilde{\gamma} = 10$ .

## References

- [1] H. B. G. Casimir, Proc. Kon. Nederl. Akad. Wet. **51**, 793 (1948).
- [2] E. M. Lifshitz, Sov. Phys. JETP (USA) **2**, 73 (1956).
- [3] P. W. Milonni, *The Quantum Vacuum* (Academic Press, San Diego, 1994).
- [4] M. Krech, *The Casimir Effect in Critical Systems* (World Scientific, Singapore, 1994).
- [5] E. Elizalde, *Ten Physical Applications of Spectral Zeta Functions* (Springer-Verlag, Berlin, Heidelberg, 1995).

- [6] V. M. Mostepanenko and N. N. Trunov, *The Casimir Effect and Its Applications* (Clarendon Press, Oxford, 1997).
- [7] S. K. Lamoreaux, Phys. Rev. Lett. **78**, 5 (1997).
- [8] U. Mohideen and A. Roy, Phys. Rev. Lett. **81**, 4549 (1998).
- [9] A. Roy and U. Mohideen, Phys. Rev. Lett. **82**, 4380 (1999).
- [10] A. Roy, C.-Y. Lin, and U. Mohideen, Phys. Rev. D **60**, 111101(R) (1999).
- [11] B. W. Harris, F. Chen, and U. Mohideen, Phys. Rev. A **62**, 052109 (2000).
- [12] T. Ederth, Phys. Rev A **62**, 062104 (2000).
- [13] F. Serry, D. Walliser, and G. J. Maclay, J. Appl. Phys. **84**, 2501 (1998).
- [14] V. N. Dubrava and V. A. Yampol'skii, Low Temp. Phys. **25**, 979 (1999).
- [15] E. Buks and M. L. Roukes, Phys. Rev. B **63**, 033402 (2001).
- [16] I. E. Dzyaloshinskii, E. M. Lifshitz, and L. P. Pitaevskii, Sov. Phys. Usp. (USA) **4**, 153 (1961).
- [17] C. M. Hargreaves, Proc. Kon. Nederl. Acad. Wet. B **68**, 231 (1965).
- [18] J. Schwinger, L. L. DeRaad, Jr., and K. A. Milton, Ann. Phys. (N.Y.) **115**, 1 (1978).
- [19] V. M. Mostepanenko and N. N. Trunov, Sov. J. Nucl. Phys. (USA) **42**, 818 (1985).
- [20] V. B. Bezerra, G. L. Klimchitskaya, and V. M. Mostepanenko, Phys. Rev. A **62**, 014102 (2000).
- [21] A. Lambrecht and S. Reynaud, Eur. Phys. J. D **8**, 309 (2000).

- [22] G. L. Klimchitskaya, U. Mohideen, and V. M. Mostepanenko, Phys. Rev. A **61**, 062107 (2000).
- [23] G. L. Klimchitskaya, A. Roy, U. Mohideen, and V. M. Mostepanenko, Phys. Rev. A **60**, 3487 (1999).
- [24] R. Golestanian and M. Kardar, Phys. Rev. Lett. **78**, 3421 (1997).
- [25] R. Golestanian and M. Kardar, Phys. Rev. A **58**, 1713 (1998).
- [26] V. B. Bezerra, G. L. Klimchitskaya, and C. Romero, Phys. Rev. A **61**, 022115 (2000).
- [27] G. L. Klimchitskaya, S. I. Zanette, and O. A. Caride, Phys. Rev. A **63**, 014101 (2001).
- [28] J. Mehra, Physica **37**, 145 (1967).
- [29] L. S. Brown and G. J. Maclay, Phys. Rev. **184**, 1272 (1969).
- [30] M. Bordag, B. Geyer, G. L. Klimchitskaya, and V. M. Mostepanenko, Phys. Rev. D **58**, 075003 (1998).
- [31] B. W. Ninham and J. Daicic, Phys. Rev. A **57**, 1870 (1998).
- [32] C. Genet, A. Lambrecht, and S. Reynaud, Phys. Rev. A **62**, 012110 (2000).
- [33] M. Bordag, B. Geyer, G. L. Klimchitskaya, and V. M. Mostepanenko, Phys. Rev. Lett. **85**, 503 (2000).
- [34] M. Boström and Bo E. Sernelius, Phys. Rev. B **61**, 2204 (2000).
- [35] M. Boström and Bo E. Sernelius, Phys. Rev. Lett. **84**, 4757 (2000).
- [36] V. B. Svetovoy and M. V. Lokhanin, Mod. Phys. Lett. A **15**, 1013 (2000); 1437 (2000).
- [37] V. B. Svetovoy and M. V. Lokhanin, Phys. Lett. A **280**, 177 (2001).

- [38] S. K. Lamoreaux, e-print quant-ph/0007029.
- [39] L. D. Landau and E. M. Lifshitz, *Electrodynamics of Continuous Media* (Pergamon Press, Oxford, 1960).
- [40] M. Born and E. Wolf, *Principles of Optics* (Pergamon Press, Oxford, 1980).
- [41] M. Bordag, B. Geyer, G. L. Klimchitskaya, and V. M. Mostepanenko, Phys. Rev. D **60**, 055004 (1999).
- [42] J. C. Long, H. W. Chan, and J. C. Price, Nucl. Phys. B **539**, 23 (1999).
- [43] M. Bordag, B. Geyer, G. L. Klimchitskaya, and V. M. Mostepanenko, Phys. Rev. D **62**, 011701(R) (2000).
- [44] V. M. Mostepanenko and M. Novello, e-print hep-ph/0101306; Phys. Rev. D **63**, 1150XX (2001).
- [45] B. W. Ninham, V. A. Parsegian, and G. H. Weiss, J. Stat. Phys. **2**, 323 (1970).
- [46] J. Mahanty B. W. Ninham, *Dispersion Forces* (Academic, London, 1976).
- [47] F. Zhou and L. Spruch, Phys. Rev. A **52**, 297 (1995).
- [48] M. Bordag, U. Mohideen, and V. M. Mostepanenko, Phys. Rep. (2001), to appear.
- [49] E. M. Lifshitz and L. P. Pitaevskii, *Statistical Physics, Part 2* (Pergamon Press, Oxford, 1980).
- [50] *Handbook of Optical Constants of Solids*, edited by E.D. Palik (Academic Press, New York, 1998).
- [51] I. S. Gradshteyn and I. M. Ryzhik, *Tables of Integrals, Series and Products* (Academic Press, New York, 1980).

- [52] J. Blocki, J. Randrup, W. J. Swiatecki, and C. F. Tsang, Ann. Phys. (N.Y.) **105**, 427 (1977).
- [53] M. Schaden and L. Spruch, Phys. Rev. Lett. **84**, 459 (2000).
- [54] U. Hartmann, Phys. Rev. B **42**, 1541 (1990).

Table 1: The relative temperature correction to the Casimir force between two plates in dependence of separation for different models of a metal conductivity

	Present paper		Ideal metal	Approach of [35]	Approach of [36, 37]	
$a$ (μm)	$\delta_T(F_{ss}^D)$	$\delta_T(F_{ss}^p)$	$\delta_T(F_{ss}^0)$	$\delta_T(F_{ss}^D)$	$\delta_T(F_{ss}^D)$	$\delta_T(F_{ss}^p)$
0.1	$5.16 \times 10^{-3}$	$6.60 \times 10^{-6}$	$1.57 \times 10^{-7}$	$-7.72 \times 10^{-3}$	$2.18 \times 10^{-2}$	$1.62 \times 10^{-2}$
0.3	$9.24 \times 10^{-3}$	$5.48 \times 10^{-5}$	$1.27 \times 10^{-5}$	$-3.49 \times 10^{-2}$	$2.54 \times 10^{-2}$	$1.53 \times 10^{-2}$
0.5	$1.08 \times 10^{-2}$	$2.11 \times 10^{-5}$	$9.82 \times 10^{-5}$	$-6.43 \times 10^{-2}$	$2.70 \times 10^{-2}$	$1.52 \times 10^{-2}$
0.7	$1.18 \times 10^{-2}$	$6.05 \times 10^{-4}$	$3.77 \times 10^{-4}$	$-9.41 \times 10^{-2}$	$2.83 \times 10^{-2}$	$1.54 \times 10^{-2}$
1	$1.37 \times 10^{-2}$	$2.06 \times 10^{-3}$	$1.57 \times 10^{-3}$	-0.138	$3.06 \times 10^{-2}$	$1.68 \times 10^{-2}$
3	0.136	0.123	0.117	-0.324	0.156	0.137
5	0.580	0.563	0.553	-0.185	0.602	0.577
7	1.17	1.15	1.14	$9.75 \times 10^{-2}$	1.19	1.16
10	2.08	2.06	2.05	0.556	2.11	2.07

Table 2: The relative temperature correction to the Casimir force between a lens and a plate in dependence of separation for different models of a metal conductivity

	Present paper		Ideal metal	Approach of [35]	Approach of [36, 37]	
$a$ (μm)	$\delta_T(F_{sl}^D)$	$\delta_T(F_{sl}^p)$	$\delta_T(F_{sl}^0)$	$\delta_T(F_{sl}^D)$	$\delta_T(F_{sl}^D)$	$\delta_T(F_{sl}^p)$
0.1	$6.87 \times 10^{-3}$	$6.68 \times 10^{-5}$	$3.09 \times 10^{-5}$	$-1.51 \times 10^{-2}$	$2.34 \times 10^{-2}$	$1.59 \times 10^{-2}$
0.3	$1.13 \times 10^{-2}$	$1.08 \times 10^{-3}$	$8.09 \times 10^{-4}$	$-5.76 \times 10^{-2}$	$2.76 \times 10^{-2}$	$1.62 \times 10^{-2}$
0.5	$1.56 \times 10^{-2}$	$4.33 \times 10^{-3}$	$3.63 \times 10^{-3}$	$-9.96 \times 10^{-2}$	$3.22 \times 10^{-2}$	$1.92 \times 10^{-2}$
0.7	$2.27 \times 10^{-2}$	$1.09 \times 10^{-2}$	$9.63 \times 10^{-3}$	-0.139	$3.97 \times 10^{-2}$	$2.57 \times 10^{-2}$
1	$4.13 \times 10^{-2}$	$2.91 \times 10^{-2}$	$2.67 \times 10^{-2}$	-0.189	$5.89 \times 10^{-2}$	$4.38 \times 10^{-2}$
3	0.498	0.481	0.470	-0.192	0.519	0.496
5	1.33	1.31	1.30	0.183	1.36	1.32
7	2.24	2.22	2.20	0.636	2.27	2.23
10	3.62	3.58	3.57	1.33	3.65	3.60

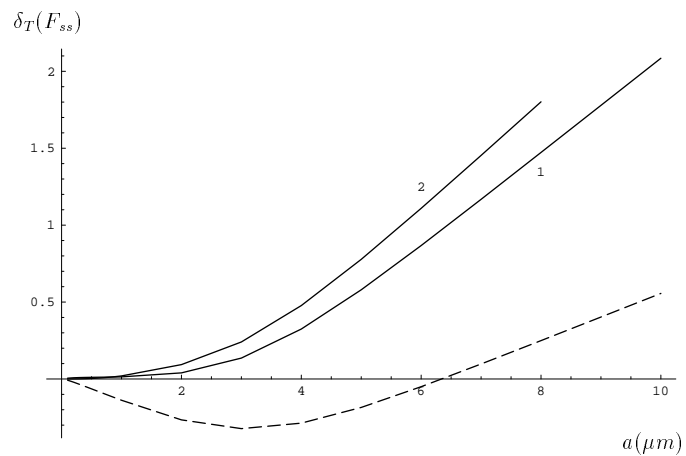


Figure 1: Relative temperature correction to the Casimir force between two plates in dependence of separation. Curve 1 corresponds to Drude model (our computation), the dashed curve is obtained in Drude model with  $r_2(0, k_{\perp}) = 0$ , and curve 2 is for the dielectric plates.

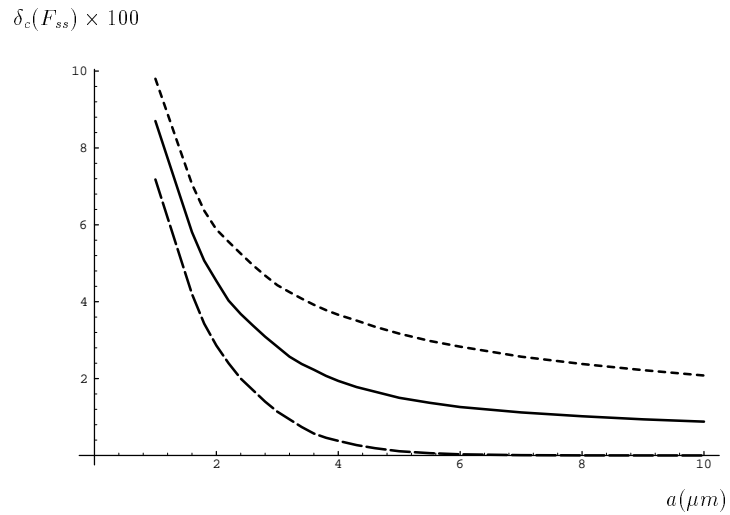


Figure 2: Relative finite conductivity correction to the Casimir force between two plates in dependence of separation in Drude model. Solid curve represents our computations at  $T = 300$  K, long-dashed curve is obtained under the supposition  $r_{1,2}(0, k_{\perp}) = 1$  at  $T = 300$  K, short-dashed curve is for  $T = 0$ .

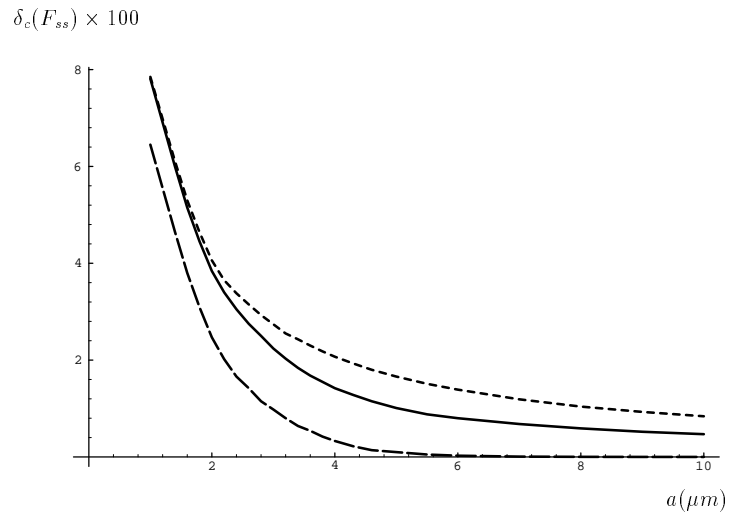


Figure 3: Relative finite conductivity correction to the Casimir force between two plates in dependence of separation in plasma model. Solid curve represents our computations at  $T = 300$  K, long-dashed curve is obtained under the supposition  $r_{1,2}(0, k_{\perp}) = 1$  at  $T = 300$  K, short-dashed curve is for  $T = 0$ .

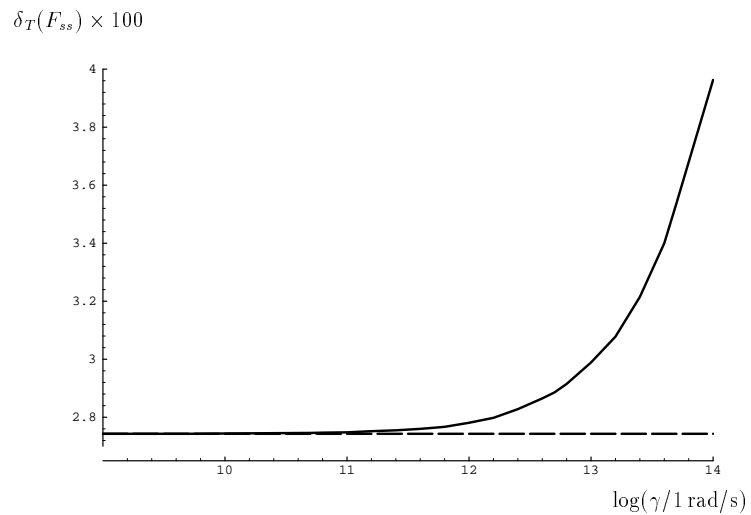


Figure 4: Relative temperature correction to the Casimir force between two plates in dependence of relaxation frequency at a separation  $a = 2 \mu\text{m}$  and  $T = 300 \text{ K}$  (solid curve). The dashed line is for plasma model.

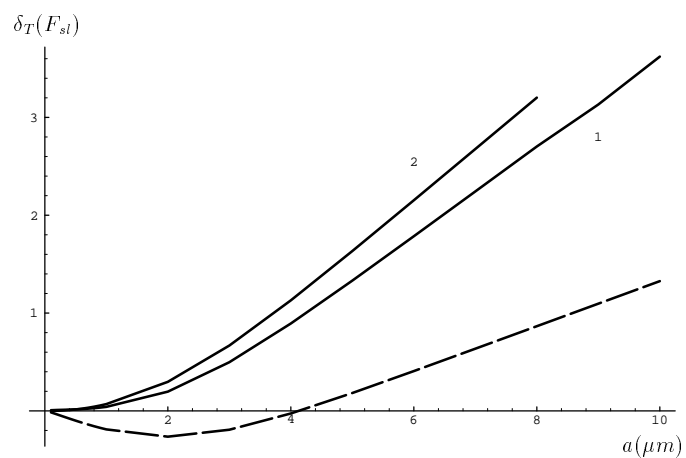


Figure 5: Relative temperature correction to the Casimir force between a plate and a lens in dependence of separation. Curve 1 corresponds to Drude model (our computation), the dashed curve is obtained in Drude model with  $r_2(0, k_{\perp}) = 0$ , and curve 2 is for the dielectric test bodies.

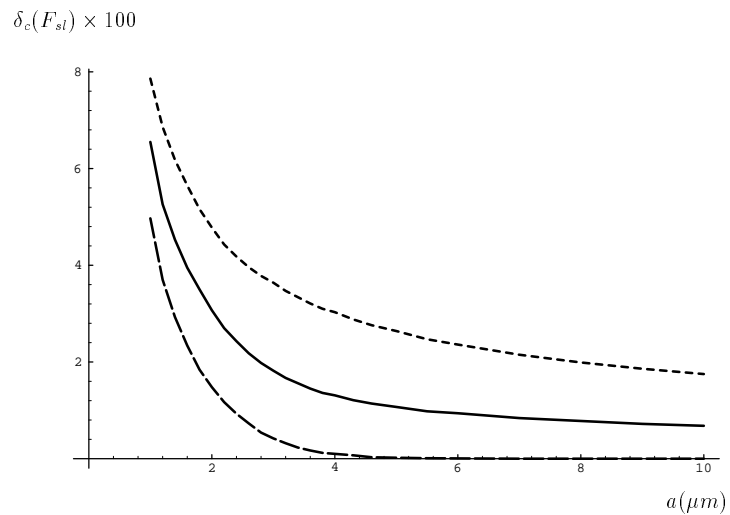


Figure 6: Relative finite conductivity correction to the Casimir force between a plate and a lens in dependence of separation in Drude model. Solid curve represents our computations at  $T = 300$  K, long-dashed curve is obtained under the supposition  $r_{1,2}(0, k_{\perp}) = 1$  at  $T = 300$  K, short-dashed curve is for  $T = 0$ .

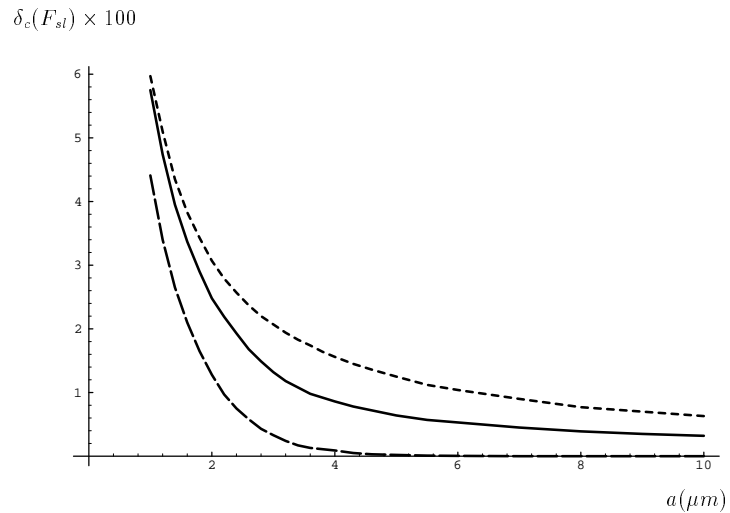


Figure 7: Relative finite conductivity correction to the Casimir force between a plate and a lens in dependence of separation in plasma model. Solid curve represents our computations at  $T = 300$  K, long-dashed curve is obtained under the supposition  $r_{1,2}(0, k_{\perp}) = 1$  at  $T = 300$  K, short-dashed curve is for  $T = 0$ .

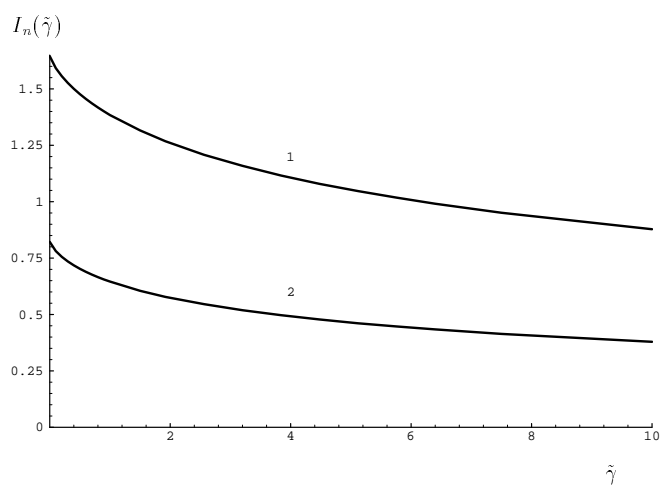


Figure 8: Dependence of the coefficient integrals in Eqs. (57) (curve 1) and (67) (curve 2) on the dimensionless relaxation frequency.